

# **Master's Thesis**

## **Hydrological Modelling for the Conservation of the Niger Inner Delta in Mali**

(マリ国ニジェールインナーデルタ保全のための水文モデリング)



**Barry KASSAMBARA**  
**GRADUATE SCHOOL OF BIORESOURCES, MIE UNIVERSITY**

**Supervisor: Prof. Takamitsu KAJISA**

**Laboratory of Water Resources Engineering**

**March, 2019**

---

# **Master's Thesis**

## **Hydrological Modelling for the Conservation of the Niger Inner Delta in Mali**

(マリ国ニジェールインナーデルタ保全のための水文モデリング)

**Barry KASSAMBARA**  
**GRADUATE SCHOOL OF BIORESOURCES, MIE UNIVERSITY**

**Supervisor: Prof. Takamitsu KAJISA**  
**Laboratory of Water Resources Engineering**

**March, 2019**

## ABSTRACT

The Niger Inner Delta (NID), a wetland that was selected as an International Important Wetland under the Ramsar Convention (on February 1st, 2004) still can be considered a hotspot of biodiversity in the Sahel. The Niger River as the main source of water for the NID is also used for urban life and irrigation. Therefore, the sustainable use of water to ensure the environmental flow in the NID is under discussion. Owing to climate change and population increase over the past three decades with a very large expansion of irrigated land upstream, the inhabitants have witnessed that their ecosystem is under threat (Cisse, 2009), and a significant reduction of its resources has occurred.

The main objective of this study is to develop different models to forecast efficiently the water-level in the Niger Inner Delta, based on the climate condition and the changing river flow.

We evaluate the performance of different models established with empirical (Artificial Neural Network and Regressions) or Conceptual Variable Source Area (Water Balance Method WBM) approaches. The results of evaluation and validation based on determination coefficient ( $R^2$ ), Root Mean Squared Error (RMSE) and Nash-Sutcliffe Efficiency (NSE) show that all the models have good results however the Lavenberg-Marquardt Artificial Neural Network (ANN) with 15 hidden layers has the best fitting for the validation and the Bayesian Regularization ANN with 80 in testing periods.

Therefore, although the WBM using Variable Source Area concept doesn't fit as well as the other models, it has the merit to estimate and forecast the wet area surrounding the water body of the delta and the monthly outflow ( $Q_{out}$ ) from the NID.

## ACKNOWLEDGEMENTS

This Thesis is submitted to Mie University as part of the courses of Environmental Science and Technology (Water Resources Engineering Laboratory), mandatory for the fulfillment of the degree of Master of Science. The project has been performed at the Department of Environment Science and Technology (Faculty of Bioresources), supervised by Prof. KAJISA Takamitsu and reviewed by Prof. SAKAI Toshinori, Prof. Zakaria HUSSEINI and Dr. OKAJIMA Kenji.

First and foremost, I would like to express my humble gratitude to all those involved in the work culminating this thesis and for taking interest in this study and sharing their knowledge. I would like to acknowledge the Malian National Board of Hydraulic for providing the valuable data.

A special thanks to Japan International Cooperation Agency (JICA) for granted me this full financial support to get a master's degree in a Japanese university through ABE program. Thanks to all the staff of JICA CHUBU and JICE for their support and kindness during my stay in Japan.

A simple word is not enough to say thank to my supervisor Prof. Takamitsu Kajisa (Kajisa Sensei) for his support, kindness, guidance and comprehension during my study

I am deeply grateful to my family for their patience and encouragements throughout the time of study fare away from home.

## LIST OF ACRONYMS

<b>AIC</b>	Akaike Information Criterion
<b>AICc</b>	Akaike Information Criterion corrected
<b>ANFIS</b>	Neuro-Fuzzy Inference System
<b>ANN</b>	Artificial Neural Network
<b>ARIMA</b>	Autoregressive Integrated Moving Average
<b>ASCE</b>	American Society of Civil Engineer
<b>Bambara</b>	Majority ethnic group in Mali working in agriculture sector
<b>BIC</b>	Bayesian Information Criterion
<b>Bozo</b>	Fishermen ethnic group in western Africa mostly in Mali
<b>BR</b>	Bayesian Regularization
<b>Dina</b>	Secular Division of the territory of Fulani Kingdom located in the Niger Inner Delta in Mali
<b>ET0</b>	Reference Evapotranspiration
<b>FAO</b>	United Nations Food and Agriculture Organisation
<b>Fulani</b>	Breeder ethnic group in western, central and eastern Africa
<b>GPR</b>	Gaussian Process Regression
<b>GRG</b>	Generalized Reduced Gradient
<b>GWP</b>	Global Water Partnership
<b>INSTAT</b>	Institut Nationale de Statistique du Mali (Malian National Institut of Statistic)
<b>IWRM</b>	Integrated Water Resources Management
<b>Jowro</b>	The ruler of the Dina

<b>LM</b>	Levenberg Marquardt
<b>Marka</b>	Ethnic group mostly working in trade and agriculture sectors
<b>MLP</b>	multilayer perceptron
<b>NASA</b>	National Aeronautics and Space Administration (United States)
<b>NBA</b>	Niger river Basin Authority
<b>NID</b>	Niger Inner Delta
<b>NSE</b>	Nash-Sutcliffe Efficiency
<b>r</b>	Correlation coefficient
<b>R<sup>2</sup></b>	Squared R
<b>RAMSAR CONVENTION</b>	An international treaty for the conservation and sustainable use of wetlands
<b>RGPH</b>	Recensement General de la Population et de l'Habitat (General Census of Population and Household)
<b>RMSE</b>	Root Mean Squared Error
<b>SAR</b>	conventional multiplicative autoregressive
<b>SCG</b>	Scaled Conjugate Gradient
<b>SIGMA</b>	The Malian national global computerized Database for hydrology survey
<b>Somono</b>	Ethnic group mostly in Mali constitute by people converted in fishery activity overs than Bozo
<b>Sonrhai</b>	Ethnic group in northern Mali working in agriculture sector
<b>SVM</b>	neural network support vector machine
<b>UNDP</b>	United Nations Development Programme

<b>VSA</b>	Variable Source Area
<b>WBM</b>	Water Balance Model
<b>WEF-NEXUS</b>	Water-Energy-Food-Ecosystem NEXUS (nexus is a latin word from nectō “bind”: the act of binding together; bond source wikipedia)
<b>WL</b>	Water-Level

## CONTENTS

ABSTRACT.....	i
ACKNOWLEDGEMENTS.....	ii
LIST OF ACRONYMS.....	iii
LIST OF FIGURES.....	viii
LIST OF TABLES.....	x
LIST OF APPENDICES.....	xi
CHAPTER I: INTRODUCTION.....	1
1.1.  MOTIVATION AND OBJECTIVE.....	2
1.2.  OVERVIEW OF THE THESIS.....	5
CHAPTER II: LITERATURE REVIEW.....	6
CHAPTER III: STUDY AREA AND DATA SOURCES.....	11
3.1.  STUDY AREA.....	12
3.1.1.  Background of Republic of Mali, Niger River and the Inner Delta in Mali.....	12
3.1.2.  Climate Conditions.....	13
3.1.3.  The Niger River and its Hydrological Potential in Mali.....	13
3.1.4.  The Niger river Inner Delta (NID).....	15
3.1.4.1.  Hydrology of the NID.....	16
3.1.4.2.  Geology and Hydrogeology of the NID.....	16
3.1.4.3.  Populations and Natural Resources of the NID.....	17
3.2.  DATA SOURCES AND DESCRIPTION.....	20
3.2.1.  The hydrometric data.....	20
3.2.2.  The Meteorological Data.....	21
3.2.2.1.  Reference evapotranspiration.....	21
3.2.2.2.  Precipitation.....	22
CHAPTER IV: METHODOLOGY.....	29
4.1.  ARTIFICIAL NEURAL NETWORK.....	31
4.1.1.  Levenberg-Marquardt Algorithm (LM).....	38

4.1.2. Bayesian Regularization Algorithm (BR).....	38
4.1.3. Scaled Conjugate Gradient Algorithm (SCG).....	38
4.2. GAUSSIAN PROCESS REGRESSION (GPR) MODEL WITH MATLAB REGRESSION LEARNER.....	39
4.3. WATER BALANCE MODEL USING VARIABLE SOURCE AREA CONCEPT .....	41
4.4. EVALUATION AND VALIDATION.....	44
4.4.1. Root Mean Squared Error (RMSE).....	44
4.4.2. The Nash-Sutcliffe Efficiency.....	44
4.4.3. Akaike Information Criterion (AIC) and Bayesian Information Criterion (BIC)	45
CHAPTER V: RESULTS.....	47
5.1. ARTIFICIAL NEURAL NETWORK.....	48
5.2. GAUSSIAN PROCESS REGRESSION (GPR) MODEL WITH MATLAB REGRESSION LEARNER.....	51
5.3. WATER BALANCE MODEL USING VARIABLE SOURCE AREA CONCEPT.....	52
CHAPTER VI: DISCUSSION.....	65
6.1. MODELS PERFORMANCE COMPARISON AFTER CALIBRATION.....	66
6.2. MODELS COMPARISON FOR PREDICTION.....	67
CHAPTER VI: CONCLUSION AND SUMMARY.....	76
6.1. CONCLUSION.....	77
6.2. SUMMARY.....	79
REFERENCES.....	81
APPENDIX.....	86

## LIST OF FIGURES

Fig. 1 : Hydraulicity of the Niger river before and after Sélingué dam construction. ....	24
Fig. 2 : Location of the Niger Inner Delta (NID) within the Niger River Basin and the hydro- Meteorological stations (Ibrahim, et al., 2017). ....	25
Fig. 3: Box Plots of Niger River flow Distribution at Mopti Station (1960 to 2015).....	26
Fig. 4: Water Level of the NID observed in Akka Station from 1960 to 2015.....	27
Fig. 5 : Box Plots of Rainfall Distribution within the Rainy Saison from 1960 to 2015 .....	28
Fig.. 6: Biological neuron.....	33
Fig. 7: Multilayer Neural Network Architecture.....	34
Fig. 8: Root Mean Squared Error by number of hidden neurons and algorithm.....	57
Fig. 9: Scatter plot of Observed versus Simulated <i>WL</i> Levenberg-Marquardt with 40 hidden layers (ANN ML).....	58
Fig. 10: Scatter plot of Observed versus Simulated <i>WL</i> Bayesian Regularization with 80 hidden layers (ANN BR).....	59
Fig. 11: Scatter plot of Observed versus Simulated <i>WL</i> Scaled Conjugated Gradient with 20 hidden layers (ANN SCG) .....	60
Fig. 12: Min objective vs Number of functions evaluation.....	61
Fig. 13:: Objective function model after optimization .....	62
Fig. 14: Scatter plot of Observed versus Simulated <i>WL</i> Gaussian Process Regression (GPR).....	63
Fig. 15: Scatter plot of Observed versus Simulated <i>WL</i> Water Balance Model (WBM).....	64
Fig. 16: Feed-Forward Neural Network Architecture for Bayesian Regularization .....	69
Fig. 17: Root Mean Squared Error for differents models after calibration .....	70

Fig. 18: Akaike Information Criterion for different models after calibration .....71

Fig. 19: Bayesian Information Criterion for different models after calibration .....72

Fig. 20: relation of water depth H and area size ratio  $A_2/A_1$ .....73

Fig. 21: Comparison between the observed incoming discharge  $Q_{in(obs)}$  and simulated outgoing discharge  $Q_{out(sim)}$ .....74

Fig. 22: Water-Level (WL) predicted with different models versus WL observed at Akka Station (2011-2015).....75

**LIST OF TABLES**

Table 1: Data types and sources ..... 23

Table 2: Similarity between the biological and artificial networks ..... 35

Table 3: Performance of ANN algorithms during training process with different hidden layers  
..... 54

Table 4: GPR Regression Matern 5/2 training parameters after optimization ..... 55

Table 5: Calibration parameters for Water Balance Model using Variable Source Area .... 56

Table 6: Performance indexes of different models during testing period (2011-2015) ..... 68

## LIST OF APPENDICES

Appendix 1: plots of Observed Maximum Water-Level (Hmax_Obs) VS Calculated Maximum Water-Level with Levenberd Marqardt (Hmax_LM) .....	I.
Appendix 2:plots of Observed Maximum Water-Level (Hmax_Obs) VS Calculated Maximum Water-Level with Bayesian Regularization (Hmax_BR).....	II.
Appendix 3: plots of Observed Maximum Water-Level (Hmax_Obs) VS Calculated Maximum Water-Level with Scaled Conjugate Gradient (Hmax_SCG) .....	III.
Appendix 4: plots of Observed Maximum Water-Level (Hmax_Obs) VS Calculated Maximum Water-Level with Gaussian Process Regression (Hmax_GPR).....	IV
Appendix 5: plots of Observed Maximum Water-Level (Hmax_Obs) VS Calculated Maximum Water-Level with Water Balance Model using Variable Source Area(Hmax_WBM).....	V
Appendix 6: Autoregression Problem with External Input with a NARX Neural Network Script for Bayesian Regularization feedforward .....	VI.
Appendix 7: Parameters of the Bayesian Regularization Neural Networks with 80 hidden layers .....	IX.
Appendix 8: Models training performance indexes .....	XI.

## **CHAPTER I: INTRODUCTION**

## 1.1. MOTIVATION AND OBJECTIVE

Water is a necessity for sustaining life and development of society, it is essential for agricultural production and food security. According to FAO Water Council, 2015 (FAO, 2015). It is the lifeblood of ecosystems, including forests, lakes and wetlands, on which the food and nutritional security of present and future generations depends on.

Since early 1970's when the Sahel region faced its first major drought of the century, the Niger Inner Delta (NID) critical Water-Level is under stress. This situation has been aggravated when the second drought occurred in 1980's, in addition to the construction of the first biggest hydro-power dam upstream in Selingue. Also, to mitigate the food insecurity in the country after the severe drought and the rapid population growth, the Malian government and its partners decided to accelerate the rhythm of the irrigation development projects mainly for paddy which continues today. All these factors lead to create a critical situation for the human and ecosystems in the surrounding area of the delta.

In 2000 the concept of Integrated Water Resources Management (IWRM) was introduced by the Global Water Partnership (GWP) (Agarwal, et al., 2000) as a process which promotes the coordinated development and management of water, land and related resources , in order to maximize the resultant economic and social welfare in an equitable manner without compromising the sustainability of vital ecosystems. Recently, a new approach emerged from FAO in support of food security and sustainable agriculture which is the *Water-Energy-Food-Ecosystem NEXUS* (WEF NEXUS). WEF NEXUS is a means to understand and manage “the complex interaction between water, energy, food and ecosystem” (FAO, 2014). The NID is one of the wetlands in the world facing a drastic challenge about climate change and a sustainable water resources management and it appear important to propose an accurate forecasting hydrologic model.

Since early times, one of the main functions of Science has been to predict future events from the knowledge acquired from the observation of past events. (Moyal, 1949), in the realm of determinism, a philosophical idea that has deeply influenced scientific thought, such predictions are made possible by inferring cause-effect relations between events from observed regularities. These strictly deterministic causal relations are then synthesized into “laws of nature”, which are utilized to make predictions. Hydrologic Model is a simplification of real-world system (e.g. surface water, soil water, wetland, groundwater, estuary) that aids in understanding, predicting and managing water resources (Wikipedia). The history of hydrological modelling ranges from the Rational Method by Mulvany Thomas J. in 1851 (Mulvany, 1851) to recent distributed physically and statistical-meaningful models (Rosenberg, et al., 2011), (Yu, et al., 2017), (Rezaeianzadeh, et al., 2014), (Özgür , 2007), (Khan, et al., 2006).....

Several hydrological models have been developed previously for the NID (Orange, et al., 2002), (Zwarts, et al., 2005), (Mahe, et al., 2009), (Kuper, et al., 2003). In recent years, with the development of Machine Learning, the attractiveness of Artificial Neural Network (ANN) for flood forecasting becomes more and more important. The use of ANNs has some advantages: first it can represent any arbitrary non-linear function given sufficient complexity of the trained network, secondly, ANNs can find relationship between different input samples and if, necessary, can group samples in analogous fashion to cluster analysis and most importantly ANNs are able to generalize a relationship from small subsets of data whilst remaining relatively robust in the presence of noisy or missing input, and can adapt or learn in response to changing environments (Dawson, et al., 2009).

The main objective of this thesis is to develop different models to forecast efficiently the Water-Level in the Niger Inner Delta, based on the climate condition and the changing river flow. Two different types of models will be considered:

- *Empirical Models (or Metric model)*, these are observation-oriented models which take only the information from the existing data without considering the features and processes of hydrological system and hence these models are also called data driven models. We will use the Artificial Neural Network method with three (03) different algorithms (Levenberg-Marquardt, Bayesian Regression and Scaled Conjugate Gradient) and a statistically based regression methods using Gaussian Process.
- *Physically based model*, which is the mathematically idealized representation of the real phenomenon, like the Water Balance Model using Variable Source Area (VSA) approach. Unlike the Empirical Models, VSA describe the transport of water inside the catchment and allow also to evaluate the wet area surrounding the water body.

## 1.2. OVERVIEW OF THE THESIS

The goal of this thesis is to provide solutions to one of the challenges associated to the conservation of the ecosystem in the Niger Inner Delta (NID), which is highly vulnerable to the climate change and availability of water resources. The specific challenge that were addressed in this work is to develop, compare and propose an accurate hydrological model for the NID's Water-Level forecasting with the least data available like the incoming water flow from upstream, the rainfall and the air temperatures. The thesis is organized as follows:

In chapter 2 reviews the previous work upon which our research draws. At its lowest abstraction, our work is an instance of Conceptual/Physical and Statistical/stochastic modelling apply to forecast the water level in the Niger Inner Delta. We will start from the historical evolution of physical based hydrological modelling to the recent use of Machine Learning for Statistical/stochastic approaches.

In Chapter 3 we describe the study area and the data sources, from the background of the Niger River and its potential in the Republic of Mali to the natural resources, climate, geology and hydrogeology of the Niger Inner Delta.

In Chapter 4 concerns the methodology, we begin by presenting a functional overview Artificial Neural Network, The Gaussian Process Regression concepts apply in Hydrological modelling and the alternative Water Balance Model using the concept of Variable Source Area.

In Chapter 5 the results of different hydrological models presented in chapter 4 will be given and these results will be discussed according to different statistical indexes (criteria) in Chapter 6 with the evaluation of the models for forecasting with the unused dataset (2011-2015) for the models' calibration.

## **CHAPTER II: LITERATURE REVIEW**

The benchmark of the hydrological modelling goes back to early 17<sup>th</sup> century in Great Britain with Edmond HALLEY (1686). Halley. published two papers in 1687 and 1691 which were concerned with the estimation of evaporation and the relation of evaporation to the hydrological cycle. Halley appears to have been the first to add an estimation of the evaporation part of the hydrological cycle unlike the previous procedure of comparing only rainfall and runoff (Halley, 1686).

As in the case of Edmond Halley, John Dalton (1766-1840) cited by (Dooge, 1974), is remembered in History of Science for accomplishments unconnected with the theory or practice of hydrology. Dalton by his estimates of rain (P) and Dew (D) on the one hand and river discharge (Q) and evaporation (E) on the other, obtained a tentative water balance for England and Wales. Such a water balance may be expressed in the form  $(P + D) - (Q) - (E) = S + B$ . Where S is the change of water storage and B is a residual lack of balance which arises from errors in the estimation.

In February 1851, Thomas John Mulvany presented a paper to the Institution of Civil Engineering of Ireland entitled '*On the Use of Self registering Rain and Flood Gauges in Making Observations of the Relation of Rainfall and Flood Discharges in a given Catchment*' (Mulvany, 1851). This paper contains a clear formulation of the concept of time of concentration and of the method of estimating the peak discharges which came to be known as the Rational Method. The main contribution of Mulvany to the concept of hydrological cycle is to go beyond the water balance based.

According to Horton's (1933) when rainfall intensity exceeds infiltration or storage capacity resulting in overland flow all over the basin (Horton, 1933). This is the classical version and is thought to have considerable relevance in areas of low vegetation cover and high rainfall intensity.

Also, he found that there is a close relation between total infiltration and water-losses, or water utilized directly or indirectly by vegetation, and total infiltration appears to be the best available basis of estimating “the effective rainfall” in relation to vegetation.

Rosenberg et al (2011) developed and applied a hybrid approach by combining physically based predictors variable with statistically based prediction methods to forecast seasonal streamflow in California’s three (03) hydrologic regions (Rosenberg, et al., 2011).. The hybrid forecasts are shown to attain the skill comparable to those based on observed data when a select number of predictor variables are employed, and superior skill when a full set of simulated data are considered.

YU et al. evaluated the Autoregressive Integrated Moving Average (ARIMA) for water level forecasting in the middle reach of the Yangtze River (Yu, et al., 2017). The ARIMA model accuracy decreases as the forecasting period is extended. ARIMA is a simple way and it can provide an effective way only for short term water level forecasting.

Khan et al. used the neural network support vector machine (SVM) to predict the water level of the lake in Erie North America (Khan, et al., 2006). The result shown that the SVM is somehow competitive with the multilayer perceptron (MLP) and the conventional multiplicative autoregressive (SAR) with less parameters. However, the SVM learn the physics of the system, not only from the historical data but also from its own knowledge that is learned from the recent time; this may give some distorted image of the physics of the system.

LEE et al. used the Variable Source Area concept of the rainfall-runoff process (Lee, et al., 1976). This model depicts the generation of surface runoff and can be incorporated in a rainfall-direct runoff model and provide a workable compromise between the distributed models and lumped models. This model needs at least 5 routing parameters to be estimate and depend on the mean

slope, the distribution of drainage area, the geomorphology characteristics and watershed conditions. Its implementation may be difficult where there is lack of such data.

(Wolock, 1993) simulated the Variable-Source-Area concept of streamflow generation with the watershed model TOPMODEL. TOPMODEL requires the specification of soils and topographic parameters, watershed latitude and time series of precipitation and air temperature. The advantage of TOPMODEL is that in addition to streamflow, estimates overland and subsurface flow and the spatial pattern of the depth to the water table in the watershed.

(Zadeh, et al., 2010). used Artificial Neural Network (ANN) models to predict daily flows from Khosrow Shirin (Iran) Two activation functions: logistic sigmoid and tangent sigmoid. The Levenberg Marquardt (LM) algorithm was used to train the models and as result the tangent sigmoid has the best fitting in validation with  $R^2=0.89$  and  $RMSE=1.7m^3/s$ . Therefore, this study doesn't considered others training algorithm like Conjugate Gradient, Cascade correlation etc for error minimization and training optimization except LM.

(Govindaraju, 2000) under the American Society of Civil Engineering (ASCE) task Committee on Application of Artificial Neural Networks in Hydrology published two series of paper on the role of ANN in Hydrology. The two series concern the preliminary concepts (Govindaraju, 2000) and the application in hydrology. These papers show the strengths and limitations of ANN and bring out the similarities they have with other modelling approaches, such as the physical models.

(Özgür , 2007) made a comparison between different Artificial Neural Network (ANN) algorithms ( Levenberg\_Marquardt, Conjugate Gradient, Cascade Correlation ) to forecast the daily streamflow of the North Platte River in United States. The result indicate that the Levenberg\_Marquardt algorithm gave the best result.

(Ogilvie, et al., 2015) presented a semi-automated method exploiting 526 MODIS (Moderate Resolution Imaging Spectroradiometers) 8-days 500m images to study the spatial and temporal dynamics of annual flood across the Niger Inner Delta over the period 2000-2011. They found that the flooded area varied between 10 300 km<sup>2</sup> and 20 000 km<sup>2</sup>, resulting in evaporation losses ranging between 12 km<sup>3</sup> and 21 km<sup>3</sup>.

(Ibrahim, et al., 2017) used the water balance analysis for spatio-temporal dynamics of the flooded area and water losses over the Niger Inner Delta (NID). He found that (i)the flooded area varied between 25,000 km<sup>2</sup> in wet period and 2,000 km<sup>2</sup> in dry period, (ii) the precipitation's contributions to the NID water budget represents 12,8% of the total inflow.

**CHAPTER III: STUDY AREA AND DATA SOURCES**

### 3.1. STUDY AREA

#### 3.1.1. Background of Republic of Mali, Niger River and the Inner Delta in Mali

The Republic of Mali is a landlocked country in West Africa; it is the eighth-largest country in Africa, with an area of 1,241,190 km<sup>2</sup> and a population of approximately 17.8 million (INSTAT, 2015). According to the UNDP report (2015), 50.6% of the population lives below the income poverty line (\$1.25/day), and 10.8% lives in near-multidimensional poverty (Programme, 2015). With 80% of its population engaged in agricultural activities, this sector is the cornerstone of Mali's economy and shows great potential to drive economic growth. Over 31% of the population is exposed to food insecurity (INSTAT-MALI, 2016); however, only 7% of 43.7 million hectares of arable land is currently cultivated. Potential irrigable lands that are currently developed correspond to 2.2 million hectares or 14% of the total (Adama, 2008).

Approximately half of Africa's total wetland area comprises floodplains. These include famous large-scale examples, such as the Niger Inner Delta (NID) in Mali, the Okavango Delta in Botswana, the Sudd of the Upper Nile in Sudan and the Kafue Flats in Zambia, that cover several thousand square kilometers (Lemly, et al., 2000).

In the 1960s, the independent countries of the Niger Basin decided to coordinate their efforts in order to manage the natural resources of the basin, among which water is the first. The Commission of the Niger River was renamed the Niger Basin Authority (NBA) November 21, 1980. The member Countries are: *Benin, Burkina Faso, Cameroon, Côte d'Ivoire, Guinea, Mali, Niger, Nigeria and Chad.*

### 3.1.2. Climate Conditions

The land-locked territory of Mali is very close to the Tropic of Cancer and it has tropical climate. It has distinct summer and winter months with three main seasons. The rainy season from June to October, the winter season between October and February, which is followed by an extremely hot and dry climate until June.

In central part of the territory where Niger Inner Delta is located, the average temperatures ranging between 24° and 32° Celsius. and mostly receives rainfall between June and August. Annual rainfall measures around 300 mm. The period of the 1960s remains rather rainy, however, a large rainfall deficit occurred in the 1970s and the 1980s, corresponding to the two great drought periods (*la grande secheresse*) in the Sahelian countries. For the more recent periods, there has been a statistical increase since the 1990s, although the level remains below the average for several years.

### 3.1.3. The Niger River and its Hydrological Potential in Mali

The Niger is the main river in western Africa, extending about 4,185 km (2,600 mi) with 1,700 kilometers (1,060 miles) in Mali (*fig. 2*). Its source driven by rainfall is located hundreds of kilometers upstream in southeastern Guinea highland. The total catchment area of the Niger River is 2,117,700 km<sup>2</sup> (817,600 sq.mi). The water discharge of Niger River fluctuates significantly, the reasons of this fluctuation are natural as well as man-made.

The Upper Niger has four dams, and three dams are currently considered for construction. The Sélingué dam on the Sankarani River is used for hydro-power since 1982 with a total volume of 2.1667 km<sup>3</sup>, an effective volume of 1.9287 km<sup>3</sup> and a design flood discharge of 3600 m<sup>3</sup>/s. The Sotuba dam, which is in operation since 1929, is another, very small hydropower plant, located directly downstream from Bamako. Because of the limited storage volume of the Sotuba dam, this

reservoir does not have a significant hydrological impact on the Niger river flow. The Markala dam, which opened in 1947, is a diversion dam just downstream of Ségou with a storage volume of 0.17 km<sup>3</sup>. This dam is used to irrigate the area of the Office du Niger. There are two diversion dams on the Bani (tributary of Niger River), Talo construct in 2007 and Djenné under construction. Talo dam have a storage volume of 0.18 km<sup>3</sup>. In addition to the existing dams, three major dams are considered for construction; the Fomi dam in Republic of guinea, the Taoussa Dam in downstream of Niger Inner Delta in Mali and Kandadji Dam in republic of Niger.

To characterize the hydrological regime of the Niger River, Koulikoro station, located about 200 km upstream from the Markala dam, was selected. This station allows to characterize the hydrology of the Niger River with an acceptable level of precision because it has been operating since 1907 with continues series of data since its establishment.

From 1907 to 1982 the data recorded in the Koulikoro station represent the natural flow of the Niger River before the construction and exploitation of Sélingué dam in 1982. The dam is located on the Sankarani River, a tributary of the Niger river, about 200 km upstream of Koulikoro. Since Sankarani River contributes significantly to water supplies in the Niger River, the dam of Sélingué regulate the flow of the Niger River and provide water to the Office du Niger and other irrigation systems downstream.

Before Sélingué dam construction, the highest monthly flow recorded is 7 586 m<sup>3</sup>/s in 1928 and after the dam construction, the highest monthly flow was recorded 2001 with a value of 5 500 m<sup>3</sup> /s. This dam is the only hydraulic structure currently used to regulate the river flow downstream. *Figure 1* describes the annual average flow variation (hydraulicity) of the Niger River in Mali since 1906 and the conditions before and after the construction of Sélingué dam.

### 3.1.4. The Niger river Inner Delta (NID)

All over the world the floodplains constitute the centers of bio-diversities and attract also many people, the NID forms no exception. Beyond the town of Ségou, the Niger River forms a vast inland delta, it's about 350 km long and 100 km wide with a surface area of 41,800 km<sup>2</sup> and constitutes the second largest delta in Africa after Okavango Delta in Botswana (Zwarts, et al., 2005). According to Gallais (1967), the NID is defined by the maximum extension of floodwaters and peripheral lakes (Gallais, 1967):

- To the east and south by the slope of Bandiagara plateau,
- To the west by the dead delta, an area of ancients' deposits above the current delta,
- To the north by a series of dunes oriented east to west

The NID forms several lakes after joins with its main tributary, the Bani, at Mopti; the watershed area of this Inner Delta covers 130,000 km<sup>2</sup> (Ibrahim, et al., 2017) as shown in *fig 2*. The major characteristic of the NID is the large variability of natural conditions between seasons and between years. This variability is due to the changes of flood level and the seasonal and annual variation of rainfall and climate conditions.

On 1<sup>st</sup> February 2004, to mark World Wetlands Day, Mali Authorities officially announced the designation of the entire NID as a Ramsar site after the Ramsar Convention Secretariat meeting in Gland, Switzerland, 23 January 2004. The NID then formed the third biggest Ramsar site in the world with an area of 4,119,500 ha (Ramsar, 2004).

#### *3.1.4.1. Hydrology of the NID*

The Niger river Inner Delta is one of the sub basins of the Upper Niger Basin; the water flowing into the NID can be observed at the Mopti hydrologic station located exactly at the meeting point between the main rivers coming from the Bani catchment area and the other sub basins of the Upper Niger. The total catchment area of the Bani (129,000 km<sup>2</sup>) is nearly as large as the rest of the Upper Niger basin upstream of the NID (147,000 km<sup>2</sup>). The flow at Mopti station results in a gradual decrease of discharge mainly due to water withdrawal for agriculture, dams, reservoirs, the climate conditions and the recharge of aquifers (groundwater). The river loses a part of its potential flow between Segou, at 900 km from its source, and Tombouctou, at 1500 km, due to evaporation caused by the hot climate and several irrigated areas like Office du Niger (Zwarts, et al., 2005), (Kassambara, et al., 2018). The water supply by the Bani tributary does not compensate for the losses and the situation is becoming worse by the construction of two dams and the extension of irrigated areas.

#### *3.1.4.2. Geology and Hydrogeology of the NID*

The Inner Delta comprises four distinct morphologic regions: the upper delta, the central delta, the lakes district, and the lower delta. In the NID, Quaternary and recent deposits mask the substratum and in particular the Eocene to Pliocene Continental Terminal. These recent deposits are either alluvial or dunelike Holocene ergs, with groundwater aquifers linked to the waterways (Andersen, et al., 2005). The Continental Terminal is a continuous stratum aquifer composed of clay-like sandstone, sand, and clays, with good water quality. Underneath the Continental Terminal and the Eocene and Cretaceous layers of these sedimentary basins lies the Continental Shale Band aquifer.

### 3.1.4.3. Populations and Natural Resources of the NID

In 1905 the population of NID was estimated to 83,500 inhabitants (Gallais, 1967) and the last General Census of the Population and the Habitat of Mali in 2009 estimated its population to 1,100,650 inhabitants RGPH,2009 (INSTAT-MALI, 2016). In one century the NID population grew by a factor of 13.

Jean Gallais, 1967 conducted an Ethnological and Geographical study in the NID. According to this study, for centuries, the natural resources of the Inner Delta were nearly divided among the people according to a traditional management system call “Dina” in which the area was divided into grazing territories as illustrated *photo 1 & 4*. The “Jowro” ruled the entire Dina territory and each sub-area were manage by a “Master of Water” and a “Master of Land”. The Master of Water managed the access to the fishing ground and the Master of Land did the same to the flood-plains when dry. In practice, the two masters managed the same area but in different seasons. The Fulani herders came with their cattle to graze in the flood-plain during the dry period, where the Bozo and Somono has been fishing some months earlier. The farmers (Marka, Bambara, Sonrhai...) planted rice in the rainy season just before the flood covered the area and harvest some months later during receding water (Zwarts, et al., 2005). After the independence of Mali from French colonial rule in 1960, the government started to build its own administration with technical services. This new control system weakened the traditional way of management and created/strengthened tensions among the growing populations as illustrated on *photo 2*. A recent research conducted by a Malian Socio-anthropologist Modibo Galy Cisse (Cisse, 2009), show clearly the increasing of tensions among villages and communities mainly due to the scarcity of natural resources. Also, some political analysts like International Crisis Group, 2016 (Int. Crisis Group, 2016). connect the recent rising of the fundamental jihadist group in the delta region even threatening the sovereignty of the

nation to this scarcity of resources This situation is exactly related to the concept written in 1833 by the British economist William Forster Llyod (LLoyd , 1833) later widely known due to an article written by the American ecologist and philosopher Garrett Hardin in 1968 (Garrett, 1968) as “*the tragedy of the commons*” . Hardin’s article has come to symbolize the degradation of the environment and the rising of conflicts to be expected whenever many individuals use a scarce resource in common without taking care about the interest of others.

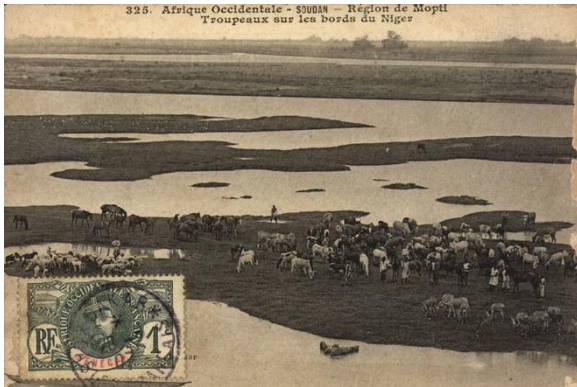


Photo 1: The Niger Inner Delta at the dawn of the French Colonial rule

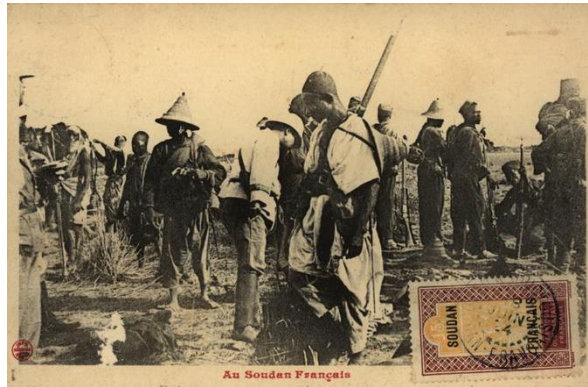


Photo 2: Disarmament of the Fulani by French army officer after one of the uprising against their secular way of land management of the NID (Dina)

*(Fortier, 1915)*



Photo 3: Transport boat in the Delta



Photo 4: Livestock breeding (Source IRD)

*(Warburton-Lee, et al.)*

### 3.2. DATA SOURCES AND DESCRIPTION

The conclusion that this study presents are based on the measurements from 1960 to 2015 of the Niger river flows at Mopti Hydrometric Station, the Water-Level at Akka Station located in the middle of the NID and the climate data from the Meteorological Station of Mopti (see *table 1*). The large area of the Niger Delta has only few hydro-meteorological stations and the spatial coverage is coarse, for some of them there are many missing data or not accessible easily; also, the hydrogeological historical data series were not available.

The structure and limitations of these data strongly influence the choice of the methods used. This section, which describes the data, is a necessary prelude to the methodology below.

After the data collection, we proceed to its preparation; this step is very important to create a successful model particularly in the case of this study where some of the data were collected manually by operators in-situ with many missing or mistake. Once the data is collected, its condition was assessed, including looking for the trends, outliers, exceptions, incorrect, inconsistent.

#### 3.2.1. The hydrometric data

The hydrometric data are from two gauges station, one located in the entrance of the NID at Mopti (14°30'N, 04°12'W) for the Inflow ( $Q_{in}$ ) the second in the middle of the NID at Akka (15°24'N, 04°14'W) for the Water-Level ( $H_{max}$ ). The Mopti gauge station was installed in 1943 by the agriculture company Office du Niger and Akka gauge station in 1955 (Marieu, et al., 1998). The observations are made daily by the Malian Government Hydraulique Board and recorded in SIGMA the national global computerized Database for hydrology survey.

From the *fig 3*, the distribution of the flow observed in the Mopti station from 1960 to 2015 is emphasized. We observed a high variability throughout the year, with a very low flow observed during the dry season (from February to June) and a medium flow in January and July. The high flow started in August and ended in December. In January, February, March, June and December, the flow has varied among the positive quartile; and the other months among the negative quartile.

The Water Level (WL) of the NID are driven mainly by the Inflow from the Upper Niger Basin (observed in Mopti) and the evapotranspiration due to extreme temperature. The amount of rainfall in the watershed is very small with an annual average ranging between 250 and 350 mm. With a gauge datum in Akka of 258.36 m<sup>+</sup> above sea level, we observed a significant variation of Water Level (see *fig 4*). The maximum WL varied from 264.38 m<sup>+</sup> in 1960's to 262.23 m<sup>+</sup> in 2010's with a depletion in the beginning of 1980's due to the century drought in the Sahelian region.

### **3.2.2. The Meteorological Data**

Meteorological data in terms of precipitation and air temperature are required inputs to the models. The data are retrieved from the Malian Meteorological Service (precipitation) and the website of Atmospheric Science Data Center of NASA (air temperature). (Kusterer, et al.)

#### *3.2.2.1. Reference evapotranspiration*

The reference evapotranspiration (ET<sub>0</sub>) is acquired input to the models in term of monthly averages. The Blaney Criddle equation is used to compute ET<sub>0</sub> (see eq.1) because it is a simplistic method when only air temperature datasets are available. When sufficient meteorological data are available The Penman-Monteith equation is usually preferred.

$$ET_0 = p(0.457 T_{mean} + 8.128) \quad (1)$$

Where:

$ET_0$  is the monthly reference evapotranspiration [mm/day]

$T_{mean}$  is the mean daily air temperature [°C] given as  $T_{mean} = (T_{max} + T_{min})/2$

$p$  is the mean daily percentage of annual daytime hours.

#### 3.2.2.2. Precipitation

Throughout the large area of the Niger inner Delta, we got the precipitation from only one gauging station, from which the dataset covers the period of our study (1960 to 2015). The *fig 5* show that from 1960 to 2015 the rainfall has the higher distribution in June, July and August; it varies among the positive quartile in May, June, September and October and among the negative quartile in July and quiet equal variation in August.

Table 1: Data types and sources

	Station	Source	Date	Data type
1	Mopti	DNH	1960-2015	Water Flow
2	Mopti	DNH		Water-Level
3	Mopti	DNM		Rainfall
4	Akka	ASDC/NASA		Air Temperature.,

*Note: DNH: Malian National Hydraulic Board, DNM: Malian National Meteorology Board, NASA: Atmospheric Science Data Center of NASA*

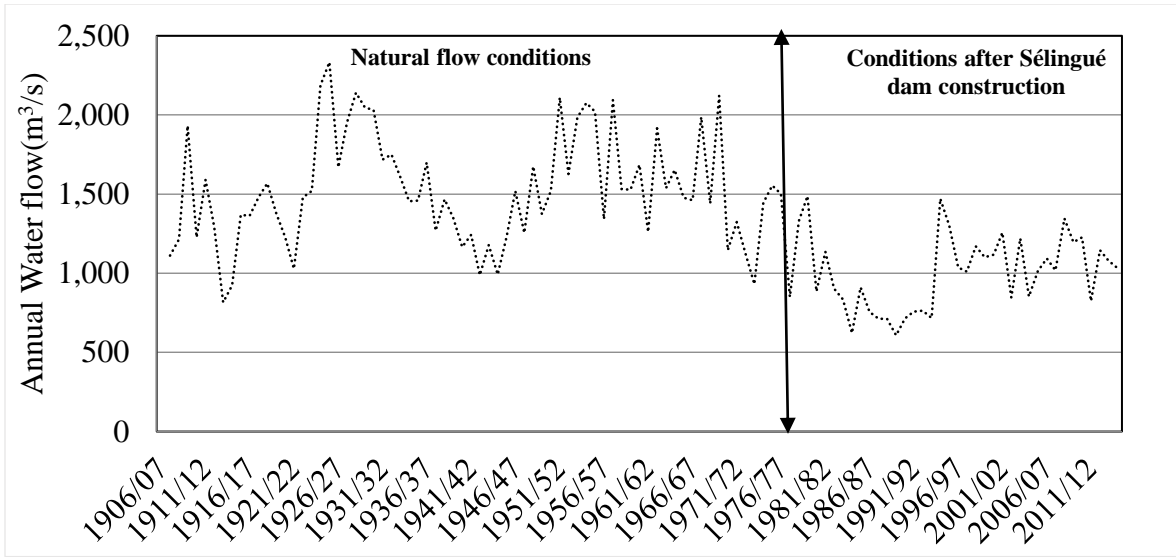


Fig. 1 : Hydraulicity of the Niger river before and after Sélingué dam construction.

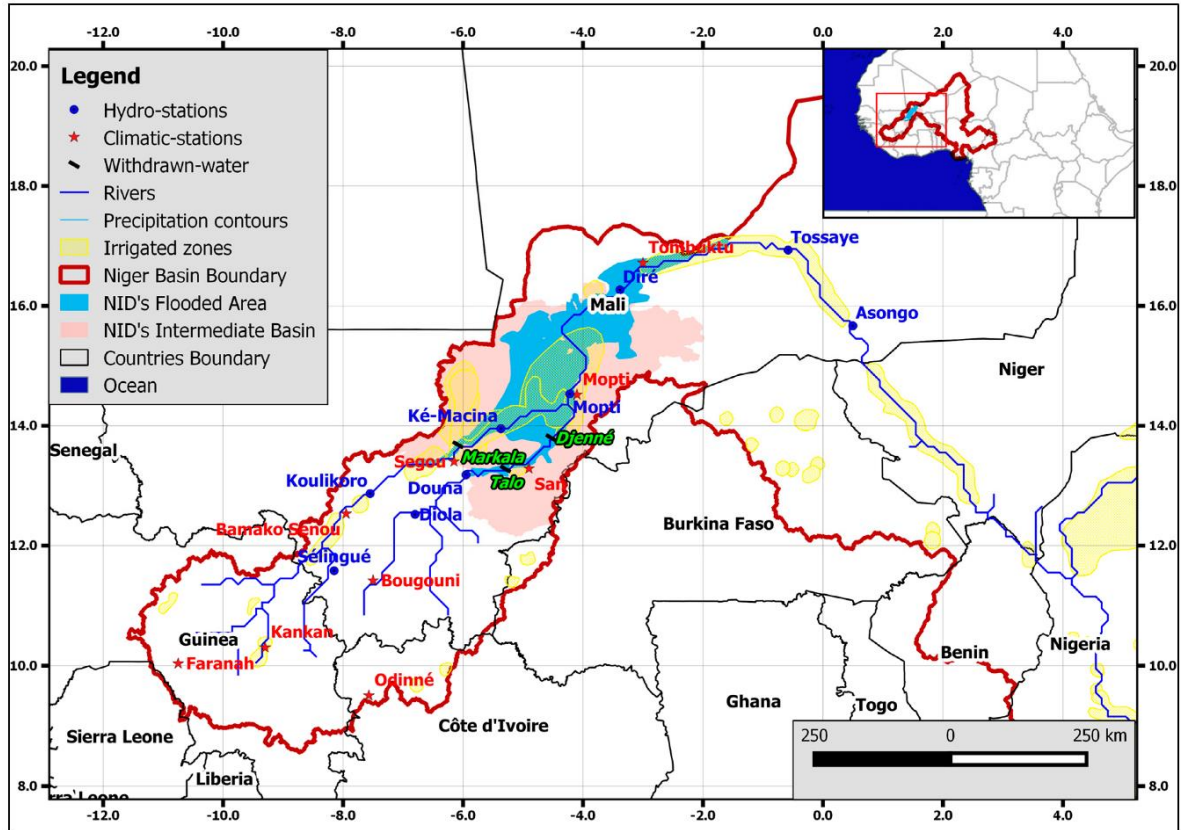


Fig. 2 : Location of the Niger Inner Delta (NID) within the Niger River Basin and the hydro-Meteorological stations (Ibrahim, et al., 2017).

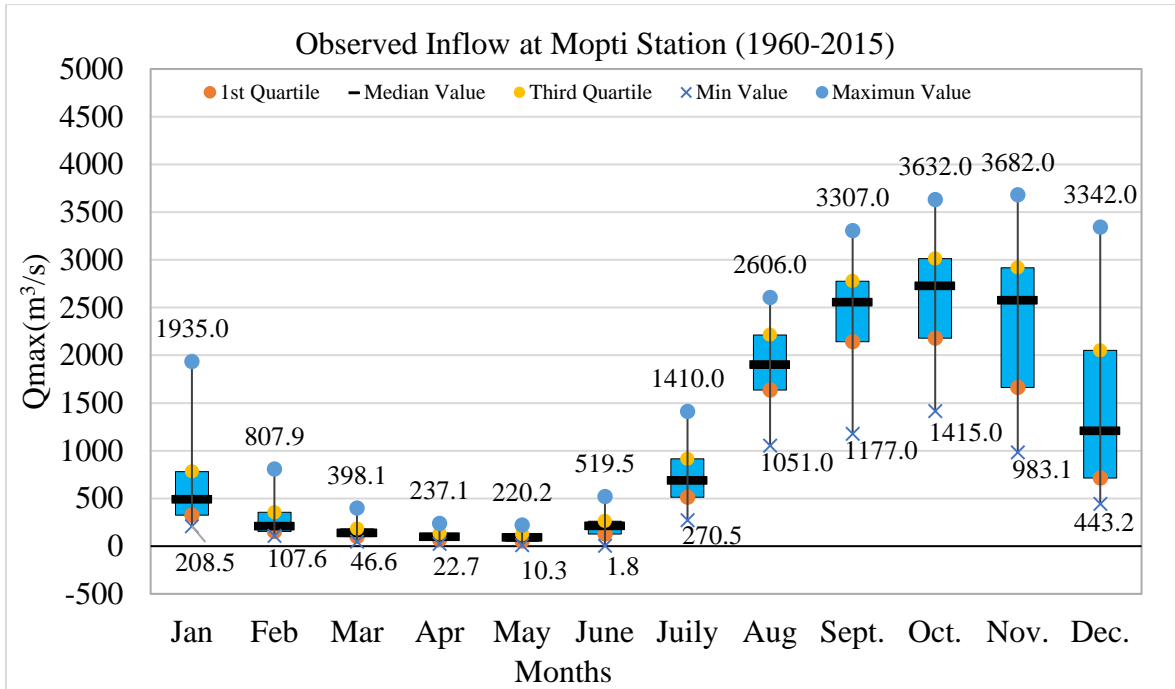


Fig. 3: Box Plots of Niger River flow Distribution at Mopti Station (1960 to 2015)

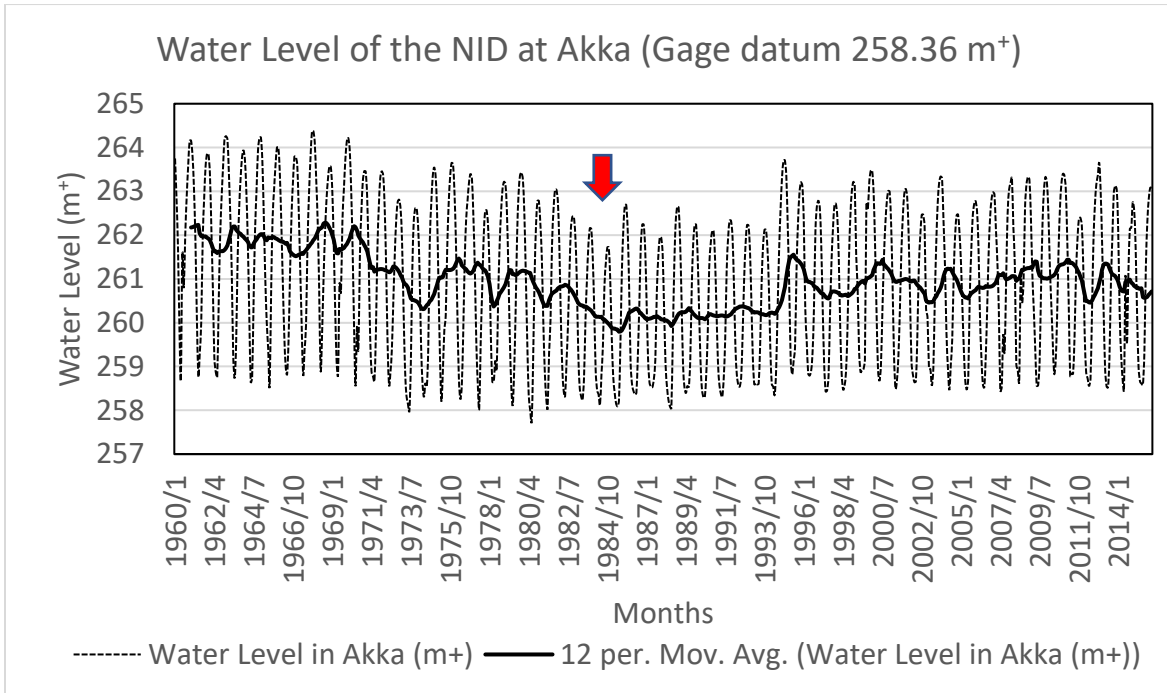


Fig. 4: Water Level of the NID observed in Akka Station from 1960 to 2015.

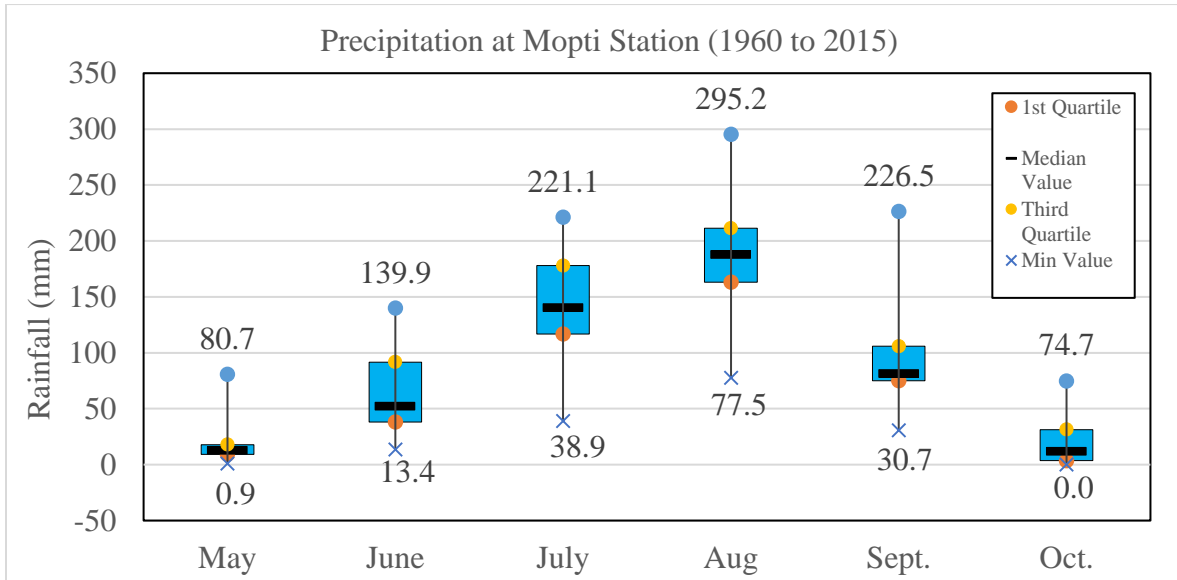


Fig. 5 : Box Plots of Rainfall Distribution within the Rainy Saison from 1960 to 2015

(Mopti Station)

## **CHAPTER IV: METHODOLOGY**

The most common methods for Niger river flow and Water Level forecasting are physical, conceptual and/or statistical rainfall-runoff methods (Ibrahim, et al., 2017), (Rezaeianzadeh, et al., 2014). In recent years Artificial Intelligence (AI) as a modern approach for data series analysis has received a great deal of attention for hydrology modeling, including Artificial Neural Network (ANN), and Adaptive Neuro-Fuzzy Inference System (ANFIS) ( (Rezaeianzadeh, et al., 2014), (Risley, et al., 2005), (Dawson, et al., 2001), (Xiong, et al., 2004), (MohammadKalteh, 2013), (Dawson, et al., 2009), (Khan, et al., 2006)). For the NID Water-Level forecasting, we have implemented three (03) different models based on empirical and stochastic approaches: Artificial Neural Network Backpropagation, the Gaussian Process Regression and Water Balance using the concept of Variable Source Area.

#### 4.1. ARTIFICIAL NEURAL NETWORK

Artificial neural networks (ANN) are statistical learning models, inspired by biological neural networks (central nervous systems, such as the brain), that are used in machine learning. These networks are represented as system of interconnected “neurons”, which send messages to each other. The connections within the network can be systematically adjusted based on inputs and outputs, making them ideal for supervised learning. The summary of biological and artificial neural networks process is given below, also some correspondence in *table 2*.

##### *Biological neural networks process:*

The biological neural circuit is a population of neurons interconnected by synapses to carry out a specific function (see *fig 6*) when activated. neural circuits interconnect to one another to form large scale brain networks. The connections between the neurons in the brain are much complex than those of artificial neurons. The basic kinds of connections between neurons are synapses, chemical and electric synapses. One principle by which neurons work is neural summation – potentials at the postsynaptic membrane will sum up in the cell body. If the depolarization of the neuron at the axon goes above threshold an action potential will occur that travels down the axon to the terminal endings to transmit a signal to other neurons.

##### *Artificial neural networks process:*

The Artificial Neural Network (ANN) is made up of neurons connected to each other (see *Fig. fig 7*); at the same time, each connection of our neural network is associated with a weight that dictates the importance of this relationship in the neuron when multiplied by the input value (Torres, 2018). Each neuron has an activation function (see eq.2) that defines the output of the neuron.

Training the neural network required learning the values of parameters (weights  $w_{ij}$  and biases  $b_j$ ) iteratively adapting the connection weight, until the connection defines an input-output function that approximates the relationship between the input and output patterns of a given training data (refer to eq 3-9).

The work flow for the general neural network design process has seven (07) primary steps for more details refers to (Beale, et al., 2018):

1. Collect data
2. Create the network
3. Configure the network
4. Initialize the weight and biases
5. Train the network
6. Validate the network (post training analysis)
7. Use the network

Step 1 might happen outside the framework of neural Network toolbox software, but this step is critical to the success of the design process.

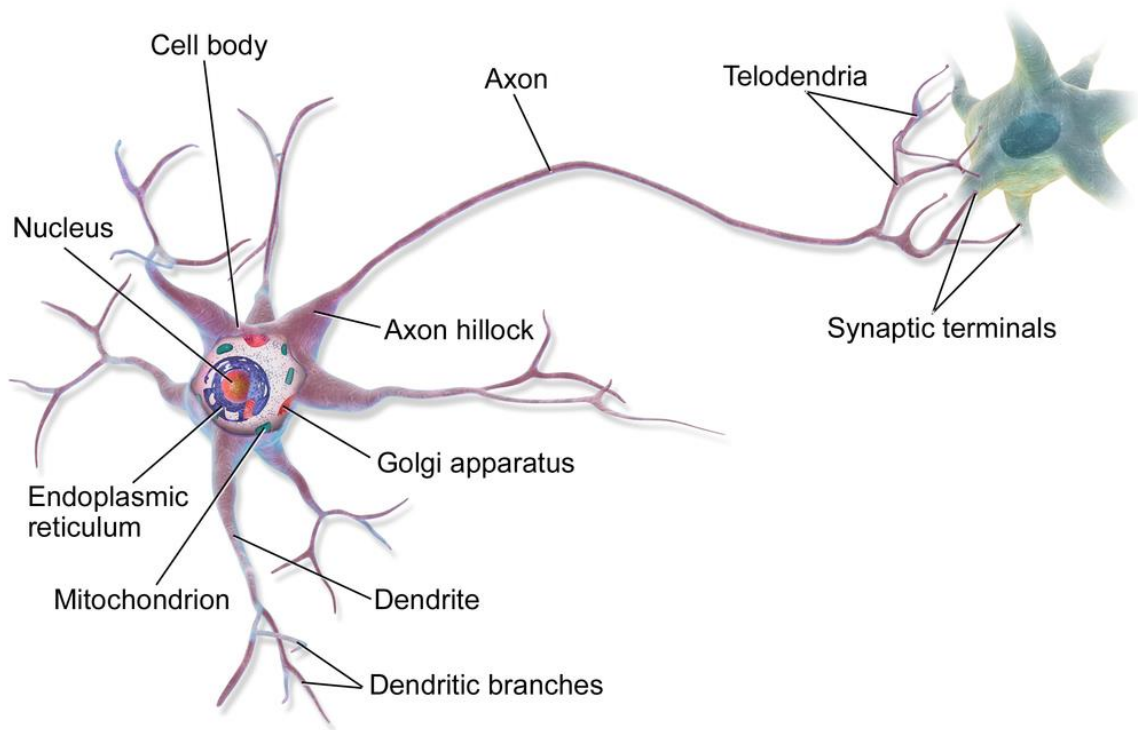


Fig.. 6: Biological neuron

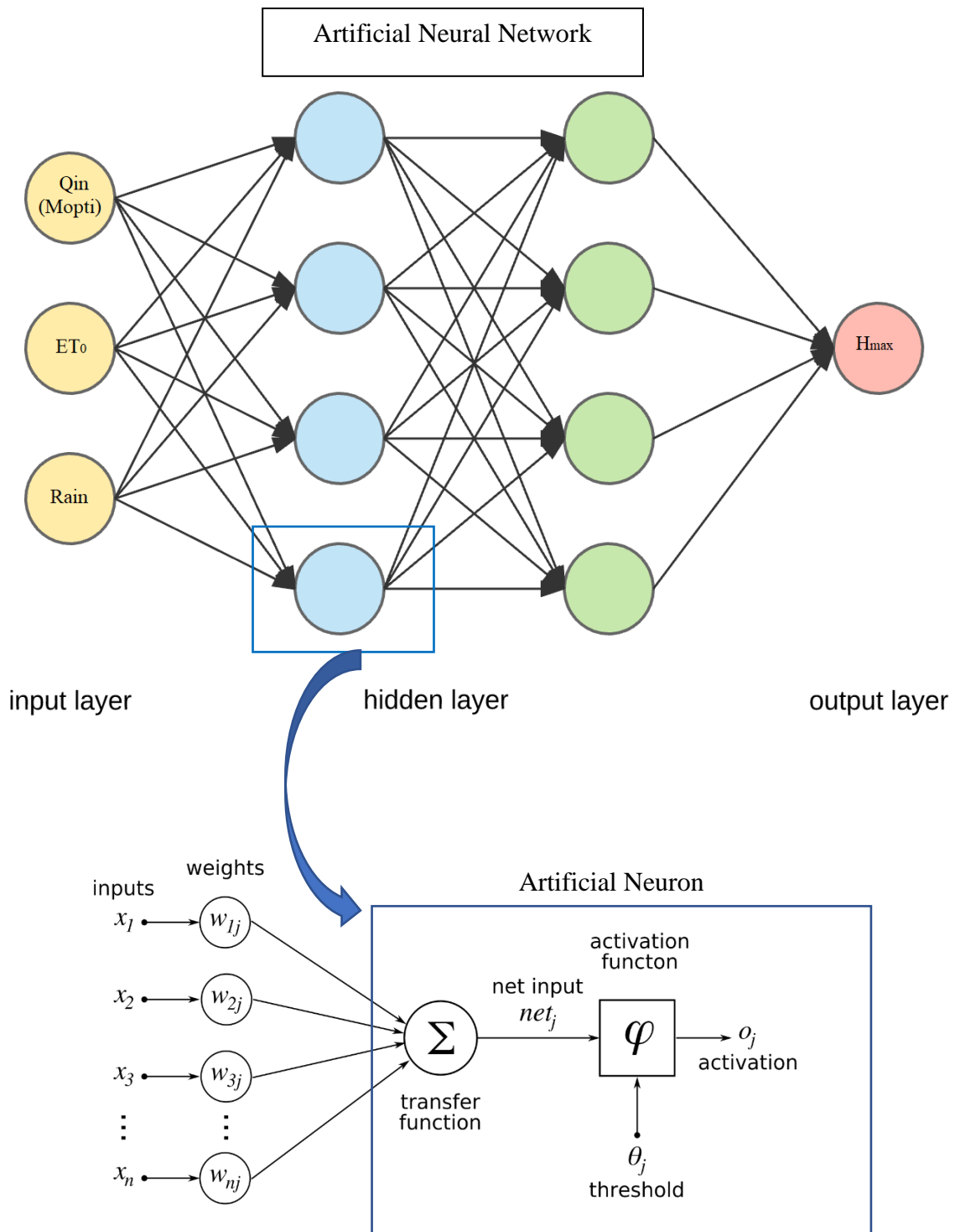


Fig. 7: Multilayer Neural Network Architecture

Table 2: Similarity between the biological and artificial networks

<b>Biological Neural Networks</b>	<b>Artificial Neural Networks</b>
Stimulus	Input data
Receptors (dendrites)	Input Layer
Neural Net	Processing Layer(s)
Neuron (cell body)	Processing Element
Effectors (Axon)	Output Layer
Response (synaptic Terminals)	Output data and an entry

*The mathematical process of ANN*

ANN is a non-linear black box statistical/stochastic approach (MohammadKalteh, 2013); the main objective is to find the optimum architecture of an ANN that can model the relationship between input and output variables. In this study we use the MATLAB Neural Network tool<sup>®</sup> to train the different models. For each of the following ANN algorithms, the monthly rainfall, evapotranspiration and the river discharge at Mopti station were designated as predictors and the water level at Akka station as the predicted.

The most commonly used ANN structure is the feed-forward multilayer perceptron (MLP). It is a network formed by simple neurons called perceptron. The perceptron computes a single output from multiple real-valued inputs by forming combinations of linear relationships according to input weights and even nonlinear transfer functions (Rezaeianzadeh, et al., 2014).

Mathematically, the Multilayer Perceptron (MLP) can be express as:

$$y^{(k)} = f\left(\sum_{i=1}^n w^{(k)}_i h^{(k)}_i + b^{(k-1)}\right) \quad (1)$$

Where  $y$  is the compute value of the maximum monthly water-level ( $H_{\max}$ );  $w_i$  the  $i^{\text{th}}$  connection weight;  $h_i$  is the input values in each layer *for the layer k1*:  $ET_{0\_obs}$ ,  $Rain_{obs}$ ,  $Q_{\max\_obs}$ ;

$b$  the neuron bias,  $k$  the number of layer and  $f$  the activation function. Let's consider the target value of water level as  $y_{target}$ .

The Multilayer neural network could have  $L$  hidden layers and compute as following:

➤ **The forward Pass:**

Layer pre-activation for  $k > 0$  ( $h^0(x) = x$ )

$$a^k(x) = b^{(k)} + w^{(k)}h^{(k-1)}(x) \quad (2)$$

Hidden layer activation ( $k$  from 1 to  $L$ )

$$y^{(k)}(x) = f(a^{(k)}(x)) \quad (3)$$

Output layer activation ( $k = L + 1$ )

$$y^{(L+1)}(x) = g(a^{(L+1)}(x)) \quad (4)$$

Where  $g$  is the output layer activation function.

Calculating the error using squared error function

$$E = \sum \frac{1}{2} (y_{target} - y^{(L+1)})^2 \quad (5)$$

➤ **The back-forward Pass:**

The goal with backpropagation is to update each of the weights  $w^k$ , in the network so that they cause the actual output to be closer the target output, thereby minimizing the error for each output neuron and the network. For the details about the procedure refer to Marquardt & al 1963 (Marquardt, 1963). An exemple of script used in MATLAB<sup>®</sup> to train the neural network in this study is shown in *appendix 6*.

Previous studies indicated that the Levenberg-Marquardt algorithm produces reasonable results for most ANN applications (Özgür , 2007), (Rezaeianzadeh, et al., 2014). For the present study we considered three algorithms available in MATLAB<sup>®</sup>: Levenberg-Marquardt (LM), Bayesian Regularization (BR) and Scaled Conjugate Gradient (SCG) algorithms.

#### 4.1.1. Levenberg-Marquardt Algorithm (LM)

Levenberg-Marquardt (LM) is the most popular alternative to Gauss-Newton method for finding the minimum of the function  $F(x)$  that is a sum of:

$$F(x) = \frac{1}{2} \sum_{i=1}^m [f_i(x)]^2 \quad (6)$$

Let the Jacobian of  $f_i(x)$  be denoted  $J_i(x)$ , then the LM method searches in the direction given by the solution  $p$  of the equation

$$(J_k^T J_k + \lambda_k I) p_k = -J_k^T f_k \quad (7)$$

Where  $\lambda_k$  are nonnegative scalars and  $I$  is the identity matrix. (Marquardt, 1963).

#### 4.1.2. Bayesian Regularization Algorithm (BR)

This algorithm uses David MacKay's Bayesian techniques to optimize regularization which requires the computation of the Hessian matrix (MacKay, 1992). Typically, training aims to reduce the sum of squared errors  $E_D$  and the regularization adds an additional term  $E_W$  (Foresee, et al., 1997). The objective term becomes:

$$F = \beta E_D + \alpha E_w \quad (8)$$

where  $\beta$  and  $\alpha$  are the objective function parameters.

#### 4.1.3. Scaled Conjugate Gradient Algorithm (SCG)

The Scaled Conjugate Gradient (SCG) method, as most of the feedforward neural networks, is based on the gradient descent algorithm well known in optimization theory. It chooses the search direction and the step size carefully by using information from the second order approximation. This algorithm is too complex to explain in few lines for more details see (Moller, 1993).

## 4.2. GAUSSIAN PROCESS REGRESSION (GPR) MODEL WITH MATLAB REGRESSION LEARNER

Gaussian process regression (GPR) models are kernel-based probabilistic models (Rasmussen, et al., 2006). A linear regression model is described as follow:

Consider a training dataset with  $n$  observations  $D = \{(x_i, y_i) | i = 1, 2, \dots, n\}$  where  $x_i$  is the input variable and  $y_i$  the target. The principal goal is the estimation of output value  $y_*$  corresponding to the new (test) input  $x_*$ . In the Gaussian Process Regression, it assumed that the observations are noisy as

$$y_i = f(x_i) + \varepsilon \quad (9)$$

Where  $f(x_i)$  is a regression function approximated by Gaussian Process with the corresponding mean  $m(x)$  that is often null and the covariance (or kernel) function  $k(x_i, x_j)$ . Also,  $\varepsilon$  the noise that follow the Gaussian distribution  $\sim N(0, \sigma^2)$ . Thus, the form of the GPR model is as follow:

$$f(x_i) \sim GP(m(x_i), k(x_i, x_j)) \quad (10)$$

$$m(x_i) = E(f(x_i)) \quad (11)$$

$$k(x_i, x_j) = E\left(\left(f(x_i) - m(x_i)\right)\left(f(x_j) - m(x_j)\right)\right) \quad (12)$$

$$k = \begin{bmatrix} cov(x_1, x_1) & cov(x_1, x_2) & \dots & cov(x_1, x_n) \\ cov(x_2, x_1) & cov(x_2, x_2) & \dots & cov(x_2, x_n) \\ \vdots & \vdots & \dots & \vdots \\ cov(x_n, x_1) & cov(x_n, x_2) & \dots & cov(x_n, x_n) \end{bmatrix} \quad (13)$$

Considering the properties of Gaussian distribution, the marginal of  $y$  can be defined as:

$$p(y|X) = N(y|f, \sigma^2 I) \quad (14)$$

Where,  $X$  is the input dataset,  $y$  is the set of target values and  $f = [f(x_1), f(x_2), \dots, f(x_n)]$  is the value of the stochastic function  $f$  calculated for each input variable. There is a joint distribution between outputs  $y$  and  $f_*$  as below :

$$\begin{bmatrix} y \\ f_* \end{bmatrix} \sim N \left( 0, \begin{bmatrix} k(x, x) + \sigma^2 I & K(x, x_*) \\ K(x_*, x) & K(x_*, x_*) \end{bmatrix} \right) \quad (15)$$

Where  $x_*$ ,  $f_*$ , and  $I$  are the test dataset, testing outputs and identity matrix respectively. In addition,  $k(x, x)$ ,  $k(x, x_*)$ ,  $k(x_*, x)$  and  $k(x_*, x_*)$  are covariance matrices.

The GPR model was fit using Matern 5/2 kernel (covariance) function defined as:

$$K_M(x_i - x_j) = \sigma_f \left( 1 + \frac{\sqrt{5}(x_i - x_j)}{\sigma_l} + \frac{5(x_i - x_j)^2}{3\sigma_l^2} \right) \exp \left( -\frac{\sqrt{5}(x_i - x_j)}{\sigma_l} \right) \quad (16)$$

It is expected that the points with similar predictor values  $x_i$ , naturally have close response (target) values  $y_i$ . In other words, it determines how the response at one point  $x_i$  is affected by responses at other points  $x_j$ ,  $i \neq j$ ,  $i = 1, 2, \dots, n$ . Where  $\sigma_l$  is the characteristic length scale, and  $\sigma_f$  is the signal standard deviation.

To improve the GPR Regression model we optimized the hyperparameters automatically by using MATLAB<sup>®</sup> *fitrGP* function. This optimization involved the estimation of the following model parameters from the data:

- Covariance function  $k(x_i, x_j | \theta)$  parameterized in terms of kernel parameters in vector  $\theta$  (see (Simonoff, 1998))
- Noise variance,  $\sigma^2$
- Coefficient vector of fixed basis functions,  $\beta$

### 4.3. WATER BALANCE MODEL USING VARIABLE SOURCE AREA CONCEPT

Runoff may occur in a uniform basin in at least four major ways:

(a) Rainfall intensity exceeds infiltration or storage capacity resulting in overland flow all over the basin. This is the classical version of Horton's (1933) (Horton, 1933) model and is thought to have considerable relevance in areas of low vegetation cover and high rainfall intensity. However, in humid temperate areas with a vegetation cover, the measured infiltration capacities of soils are generally high in comparison with normal rainfall intensities. In this case the Horton model of basin response is not applicable.

(b) Rainfall intensity exceeds infiltration or storage capacity on a variable area of near-saturated soils. This is the basis for Betson's (1964) (Betson, 1964) partial area conceptual model in which it is recognized that the spatially variable nature of infiltration capacities and differences in moisture status at the soil surface, caused by downslope flow of water, will result in some parts of the basin being far more likely to produce infiltration excess overland flow than others. Engman & Rogowski (1974) (Engman, et al., 1974) have produced a relatively simple physically based model founded on this concept.

(c) Rain falling on stream channels and completely saturated soils. Where the latter are adjacent to stream channels (as is common) this source of overland flow contributes directly to the storm hydrograph (Dunne, et al., 1970). The zone of soil saturation may extend completely from bedrock or may build up above a relatively impermeable layer within the soil.

(d) Downslope lateral flow of saturated or unsaturated soil water. Most of this flow will be within the soil ('subsurface storm flow'), but it may locally exceed the soil storage capacity and return to

flow over the surface at much higher velocities (Dunne, et al., 1970). Subsurface flow velocities are commonly too slow to contribute appreciably to the peak of the storm hydrographs although in volume terms subsurface flow may dominate the overall response of the basin in providing the hydrograph tail and low flows. In small humid temperate basins mechanisms (b) and (c) appear to be the critical sources of storm flow, with subsurface flow making a highly significant contribution in setting up the soil water conditions prior to further storm rainfall. These processes and their characteristics are thought to explain the observed nonlinearity of runoff in response to rainfall, and any simple physically based hydrograph model must reflect

this general conceptual knowledge of the mechanisms involved. A choice is available between an infiltration rate approach to the prediction of overland flow, as in the model of (Engman, et al., 1974), and a soil storage based approach in which the infiltration rate is essentially considered to be non-limiting such that the prediction of overland flow occurs when storage capacity is exceeded. The latter approach has been adopted here both because it would appear to be more physically realistic in British basins and because it has operational advantages with respect to moisture accounting.

The water depth in the NID may be obtained using the Water Balance Model (WBM) with Variable Source Area (VSA) (eq. 18). The concept of Variable Source Area was introduced for the first time by (Hewlett, et al., 1967). (Rezaeianzadeh, et al., 2014) are also known for the contribution to the fundamental concept of the VSA. The VSA develop when the soil profile becomes saturated from below after the water table rises to the land surface.

$$H_{i+1} = \text{Max}\left(H_i + (Q_{i+1} - Q_{out})\frac{D}{A_1} + (R_{i+1} - ET_{0i+1}D)\frac{(A_1+A_2)}{A_1}, \gamma\right) \quad (17)$$

The outflow  $Q_{out}$  is given by:

$$Q_{out} = \beta \text{Max}(H_i, 0)^\alpha \quad (18)$$

The wet soil area is given as:

$$A_2 = \delta \sqrt{A_1} \quad (19)$$

Time, monthly maximum inflow from Mopti station upstream ( $Q_i$ ), monthly rainfall ( $R$ ) the daily potential Evapotranspiration ( $ET_0$ ), the number of days for each month ( $D$ ), and water surface ( $A_1$ ) data were fed into the spreadsheet. To estimate the maximum water level ( $H_i$ ) at various time steps using the eq.18-20 based on the parameters  $\alpha$ ,  $\beta$ ,  $\gamma$  and  $\delta$ . The Generalized Reduced Gradient (GRG) nonlinear solving method was used to identify the parameters in Excel Solver.

#### 4.4. EVALUATION AND VALIDATION

To validate and evaluate the models, Correlation Coefficient ( $r$ ), squared R ( $R^2$ ), Root Mean Squared Error ( $RMSE$ ) and Nash-Sutcliffe Efficiency ( $NSE$ ) were used.

The choice of a model can not only be relied on the indexes above, therefore Akaike Information Criterion ( $AIC$ ) and Schwarz Criterion or Bayesian Information Criterion ( $BIC$ ) were used to select the model based on the Sum Squared Error and number of parameters. The descriptions of each index are given bellow.

##### 4.4.1. Root Mean Squared Error (RMSE)

The Root Mean Squared Error ( $RMSE$ ) is a measure of how well the model performed. It does this by measuring the differences between predicted values and the observed (or actual) values and represent the quadratic mean of these differences. The  $RMSE$  serves to aggregate the magnitude of the errors in predictions for various times into a single measure or predictive power. The  $RMSE$  is computed as shown below in eq. 21:

$$RMSE = \sqrt{\frac{\sum_{i=1}^n (Y_i^{obs} - Y_i^{sim})^2}{n}} \quad (20)$$

Where  $Y_i^{obs}$  is the  $i$ th observation monthly WL ( $H_{max i}$ ),  $Y_i^{sim}$  is the  $i$ th simulated value of monthly WL ( $H_{max i}^{sim}$ ),  $Y^{mean}$  is the mean of observed monthly WL ( $H_{max i}^{obs}$ ), and  $n$  is the total number of observations.

##### 4.4.2. The Nash-Sutcliffe Efficiency

The Nash-Sutcliffe Efficiency ( $NSE$ ) is a normalized statistic that determines the relative

magnitude of the residual variance (“noise”) compared with the measured data variance (“information”). The *NSE* indicates how well the plots of observed versus simulated data fit (Moriassi, et al., 2007).

The *NSE* is computed as shown below in eq. 22:

$$NSE = 1 - \left[ \frac{\sum_{i=1}^n (Y_i^{obs} - Y_i^{sim})^2}{\sum_{i=1}^n (Y_i^{obs} - Y^{mean})^2} \right] \quad (21)$$

Where  $Y_i^{obs}$  is the *i*th observation monthly WL ( $H_{max\ i}$ ),  $Y_i^{sim}$  is the *i*th simulated value of monthly WL ( $H_{max\ i}^{sim}$ ),  $Y^{mean}$  is the mean of observed monthly WL ( $H_{max\ i}^{obs}$ ), and *n* is the total number of observations.

#### 4.4.3. Akaike Information Criterion (AIC) and Bayesian Information Criterion (BIC)

In 1969 Hirotugu AKAIKE introduced an estimator of the relative quality of statistical models for a given set of data call Akaike Information Criterion (*AIC*) (Akaike, 1969) *AIC* is founded on information theory. When a statistical model is used to represent the process that generated the data, the representation will almost never be exact; some information will be lost by using the model to represent the process (Akaike, 1974).. The less information a model loses, higher is the quality of that model. *AIC* deals with the trade-off between the goodness of fit of the model and the simplicity of that model.

When the sample size is small, there is a substantial probability that *AIC* will overfit. To address such potential overfitting, the corrected *AIC* (*AICc*) were developed by Hurvich and Tsai, 1989 (Hurvich, et al., 1995) : *AICc* is *AIC* with correction for small sample sizes.

In 1978 Gideon SCHWARZ presented an alternative approach to Akaike Information Criterion (Schwarz, 1978) call Bayesian Information Criterion (*BIC*) or Schwarz Information Criterion.

*Akaike Information Criterion:*

$$AIC = n * \log(SSE/n) + 2 * p \quad (22)$$

*Akaike Information Criterion corrected:*

$$AICc = n * \log(SSE/n) + (n + p)/(1 - \frac{p+2}{n}) \quad (23)$$

*Bayesian Information Criterion (BIC):*

$$BIC = n * \log(SSE/n) + p * \log(n) \quad (24)$$

Where:

*SSE*: Sum of Squared Errors for the training set;

*n*: Number of training cases;

*p*: Number of parameters (weights and biases).

## **CHAPTER V: RESULTS**

The performance of the types of model is shown in this section, the empirical models and the theoretical models. The empirical models are based on the a-posteriori knowledge (i.e measurement) which concern the Artificial Neural Networks and Regression models, the theoretical models deal with the fundamental principles of physical phenomena which are the Water Balance Model using Variable Source Area (WBM-VSA).

The monthly data from 1960 to 2010 (612 datasets) were used for the model training and validations, and the monthly data from 2011 to 2015 (60 datasets) for testing. The plot of simulated versus observed Water-Level for validation are shown in *Appendix 1-5*.

## **5.1. ARTIFICIAL NEURAL NETWORK**

Comparison between the three multilayer neural network learning algorithms has been tested to learn the correspondence between simulations and measurements water-level ( $H_{max}$ ).

During the training process it's very important to choose the best feature of hidden layer and there is still a continuing debate on the selection strategies, one area of agreement suggesting that the number of hidden neurons (layers) should be directly relate to the number of inputs and outputs (Curry, et al., 2006). Several researchers proposed many approaches to fix the number of hidden neurons in neural network (Sheela, et al., 2013), (Tamura , et al., 1997) .The approaches can be classified into constructive and pruning approaches. The constructive approach starts with undersized network and then adds additional hidden neurons. The pruning approach starts with oversized network and then prunes the less relevant neuron and weights to find the smallest size. The problems of proper number of hidden neurons are to be fixed (Li, et al., 1995). The constructive approach has been chosen to find the best hidden layer for each algorithm the result is shown in *table 3* and *fig 8*.

The performances of the learning algorithms are evaluated by comparing the number of epochs which is the number of iterations through forward pass and backward pass for all the batch size (data set) and the Root Mean Squared Error (refer to Table *table 3*). The result show that during training process, Bayesian Regularization (BR) algorithm has the best performance with the smallest  $RMSE = 37.32$  cm which is reached at the epochs 359 with 80 hidden layers, follow by Levenberg-Marquardt (LM) algorithms  $RMSE = 37.45$  cm reached at epochs 13 with 40 hidden layers and the Scaled Conjugate Gradient (SCG) has a  $RMSE = 48.61$  cm and required 50 epochs with 20 hidden layers.

At this point we can say that the BR algorithm gives more accurate results and as we used constructive approach, the trend of the error follows smoothly the increase of the number of hidden neurons compare to LM and SCG algorithm (see *fig 8*). but we must consider the fact that LM algorithm although less accurate than BR, was the fastest during training process. The choice of a best model cannot be relied only on this index; therefore, AIC and BIC indexes are been used for all the models developed, refer to the point 4.4.3 for more informations.

The architecture of the Feed-Forward Neural Network Architecture for Bayesian Regularization with 80 hidden layers is shown in *fig 16* below as example. The parameters (weights and biases) and the model algorithm are shown in *Appendix 7*.

For validation we used the same input data as for training process (i.e. from 1960 to 2010) and we choose for each algorithm the model given the smallest  $RMSE$  based on the number of hidden neurons. The objective of this study is not to evaluate the speed of training based on the epochs (iterations) therefore we didn't consider this parameter.

Figures 9-11 show the scatter plots of the observed monthly water-level versus the simulated monthly water-level for the validation. We can see from these plots that Levenberg-Marquardt algorithm with 40 hidden layers (LM\_40) and Bayesian Regularization algorithm with 80 hidden layers (BR\_80) have the same coefficient  $R^2$  but only this criterium and *RMSE* are not enough to judge a model, therefore more discussion with others criterium has been considered (see *point 6.1*).

## 5.2. GAUSSIAN PROCESS REGRESSION (GPR) MODEL WITH MATLAB REGRESSION LEARNER

For the NID Water Level prediction with Gaussian Process Regression, the Matern 5/2 was chosen as the appropriate kernel function which present the best *RMSE* over three functions (Rational quadratic, exponential, squared exponential) after training with MATLAB<sup>®</sup> Regression Learner; for more details see the eq. 10 to 17. The related parameters for the Matern 5/2 Kernel Regression were acquired and the models were optimized using MATLAB<sup>®</sup> Regression optimization function to enhance the prediction quality. The optimization required 30 iterations (or number of function evaluations with differents parameters) to reach the feasible point (see fig 12 and 13Fig. ). The estimated objective function value reach was 7.8116 which represents the loss. The values of differents parameters are shown in *table 4*.

To validate the GPR Regression optimized model we use the data from 1960 to 2010. The scatter plot of the simulated versus observed monthly maximum water-level  $H_{max}$  at Akka with the GPR Regression matern 5/2 function is shown in *fig 14*.

### 5.3. WATER BALANCE MODEL USING VARIABLE SOURCE AREA CONCEPT

The model developed here is an amalgam of Variable Source Area ideas with the water balance concept.

Monthly conceptual water balance model aims to simulate the selected hydrological processes usually by conceptualizing the catchment as an assemblage of interconnected storage through which water passes from inputs as rainfall and discharges from upstream catchments recorded at Mopti station to outputs as streamflow at the catchment outlet; the controlling equations satisfy the water balance requirement. However, the processes occurring in the watershed like infiltration and the influence of groundwater etc. were difficult to use because of lack of data, then we decided to use the Variable Source Area concept in attempting to model the response of the basin (see eq. 18-20).

The model used monthly maximum inflow from Mopti station upstream ( $Q_i$ ), monthly rainfall ( $R$ ) the daily potential Evapotranspiration ( $ET_0$ ), Number of day for each month ( $D$ ), pond water surface ( $A_1$ ) and the wet area surrounding the water body surface ( $A_2$ ), to estimate the maximum water level ( $H_i$ ) at various time steps

To calibrate the model, the Generalized Reduced Gradient (GRG) nonlinear solving method was used to identify the parameters in Excel<sup>®</sup> Solver. We assumed that the maximum value of water body surface ( $A_1$ ) is 15,900 km<sup>2</sup> according to (Zwarts, et al., 2005) corresponding to the maximum water-level (504 cm) recorded at Akka station since 1960. The values of the model calibrated coefficients are shown in Table *table 4*.

- For the outflow  $Q_{out} = 228.73 \text{Max}(H_i, 0)^{1.28}$ ,
- the wet area surrounding the water body:  $A_2 = 59.19\sqrt{A_1}$  (1)

- And finally, the Water-Level at time step (t+1):

$$H_{i+1} = \text{Max}\left(H_i + (Q_{i+1} - Q_{out}) \frac{D}{A_1} + (R_{i+1} - ET_{0i+1} D) \frac{(A_1 + A_2)}{A_1}, 0.32\right)$$

Scatter plot of Observed versus Simulated WL Water Balance Model (WBM) is shown in *fig 15* with  $R^2=0.8943$ .

Table 3: Performance of ANN algorithms during training process with different hidden layers

Hidden layers	Levenberg-Marquardt		Bayesian Regularization		Scaled Conjugate Gradient	
	<i>RMSE</i>	Best Epoch	<i>RMSE</i>	Best Epoch	<i>RMSE</i>	Best Epoch
1	59.82	18	59.72	9	61.10	27
2	56.40	38	48.55	69	57.87	24
3	48.04	36	46.58	60	60.93	29
5	48.37	9	45.21	76	52.56	34
10	46.15	15	40.50	303	51.51	25
15	39.44	28	39.90	665	56.72	25
20	45.31	6	39.91	127	<b>48.61*</b>	50
40	<b>37.45*</b>	13	37.61	296	51.10	44
80	38.10	8	<b>37.32*</b>	359	52.77	55

\*: Minimal Root Mean Squared Error

Table 4: GPR Regression Matern 5/2 training parameters after optimization

<b>Parameters</b>	<b>Symbols</b>	<b>Value</b>
characteristic length scale	$\sigma_l$	2.5609
Signal standard deviation	$\sigma_f$	443.1169
Noise variance	$\sigma$	42,64
Coefficient $\beta$	$\beta$	93.12
estimated objective function value	$\varepsilon$	7.8116

Table 5: Calibration parameters for Water Balance Model using Variable Source Area

Parameters	Symbols	Value	Equations
Coefficient for Outflow $Q_{out}$	$\alpha$	1.29	$Q_{out} = \beta \text{Max}(H_i, 0)^\alpha$
	$\beta$	228.73	
Coefficient for surrounding wet area $A_2$	$\delta$	59.19	$A_2 = \delta \sqrt{A_1}$
Water-Level at time step (t+1) $H_{i+1}$	$\gamma$	0.32	$H_{i+1} = \text{Max}(H_i + (Q_{i+1} - Q_{out}) \frac{D}{A_1} + (R_{i+1} - ET_{0_{i+1}} D) \frac{(A_1 + A_2)}{A_1}, \gamma)$

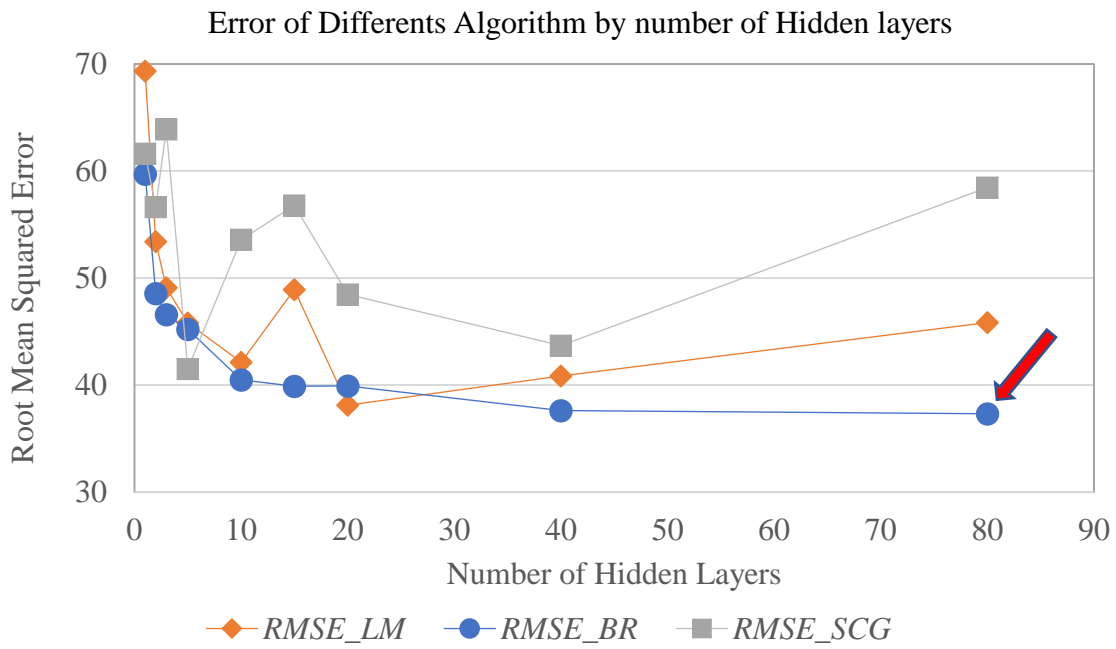


Fig. 8: Root Mean Squared Error by number of hidden neurons and algorithm

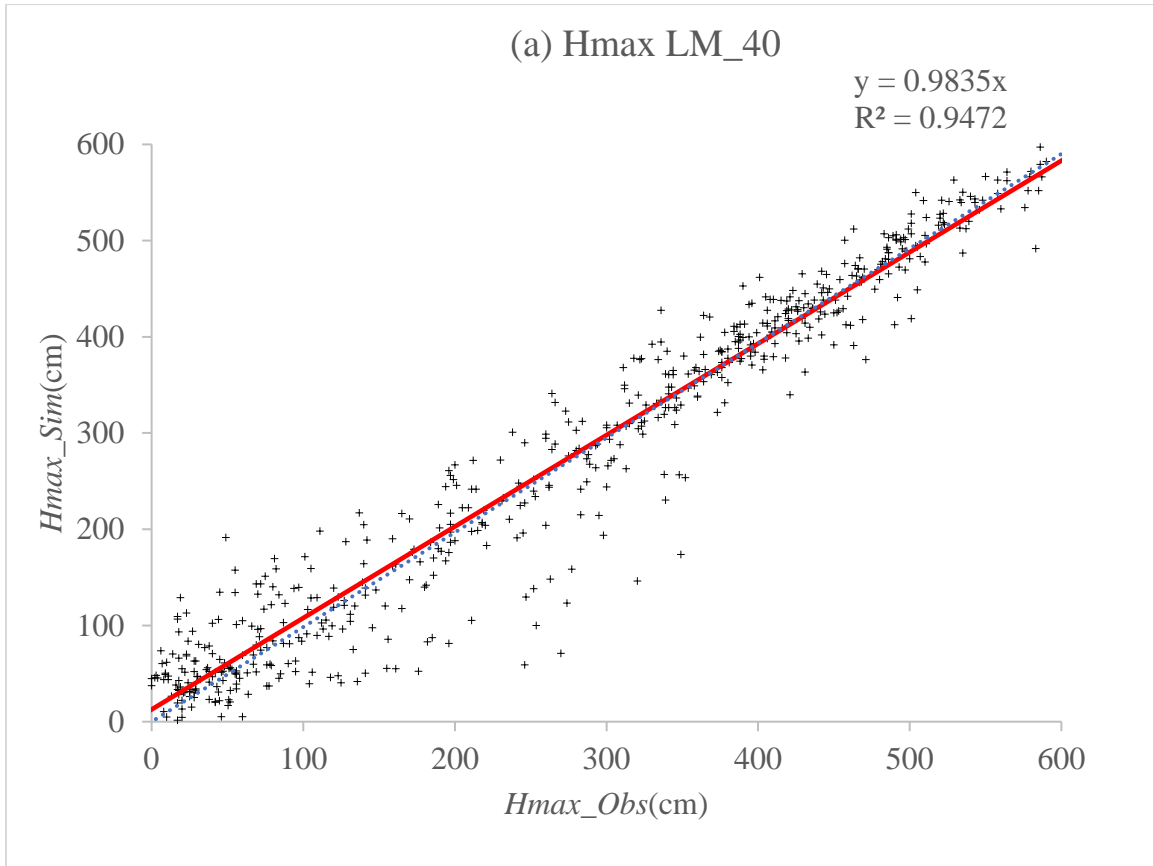


Fig. 9: Scatter plot of Observed versus Simulated *WL* Levenberg-Marquardt with 40 hidden layers (ANN ML)

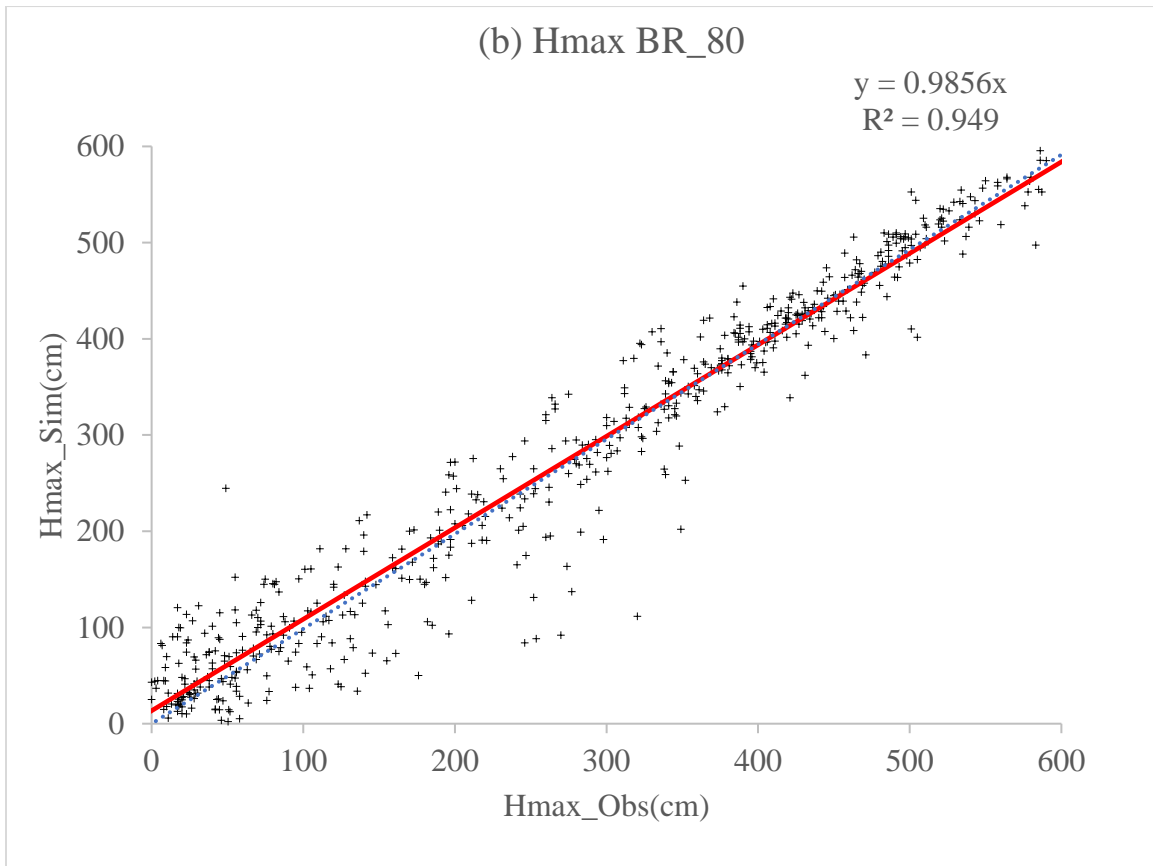


Fig.10: Scatter plot of Observed versus Simulated *WL* Bayesian Regularization with 80 hidden layers (ANN BR)

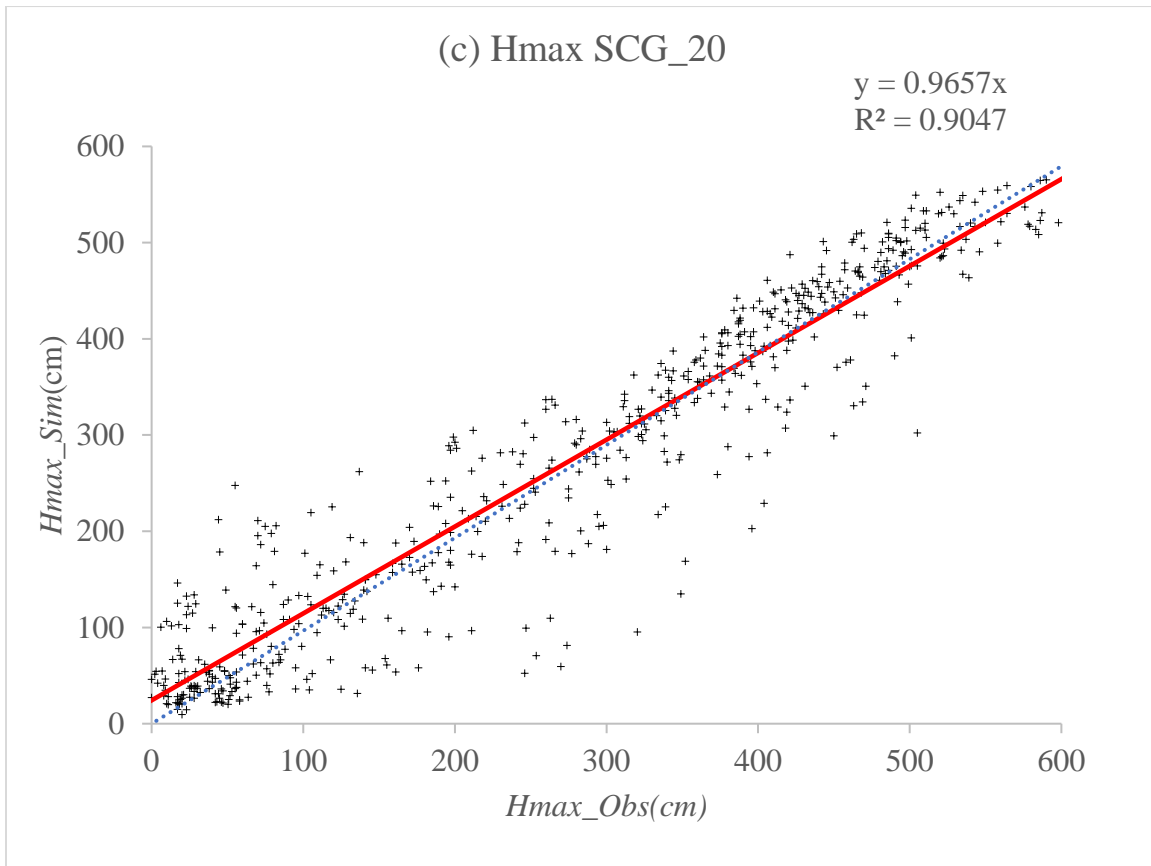


Fig.11: Scatter plot of Observed versus Simulated *WL* Scaled Conjugated Gradient with 20 hidden layers (ANN SCG)

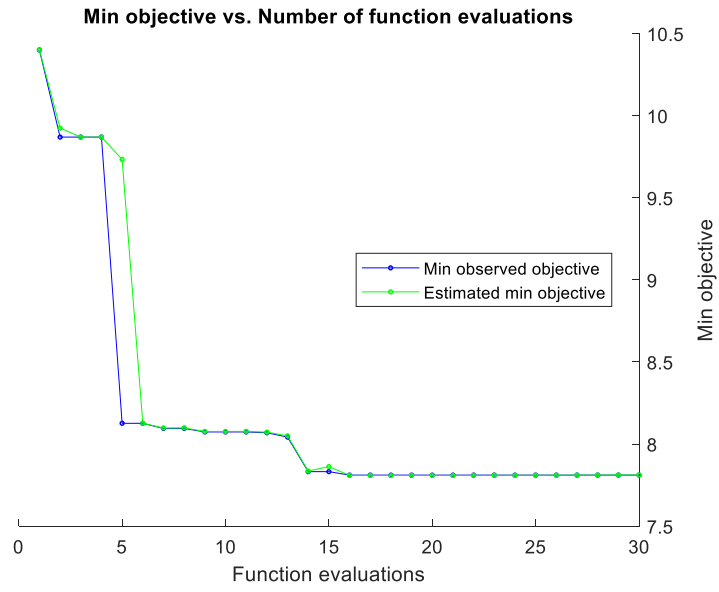


Fig. 12: Min objective vs Number of functions evaluation

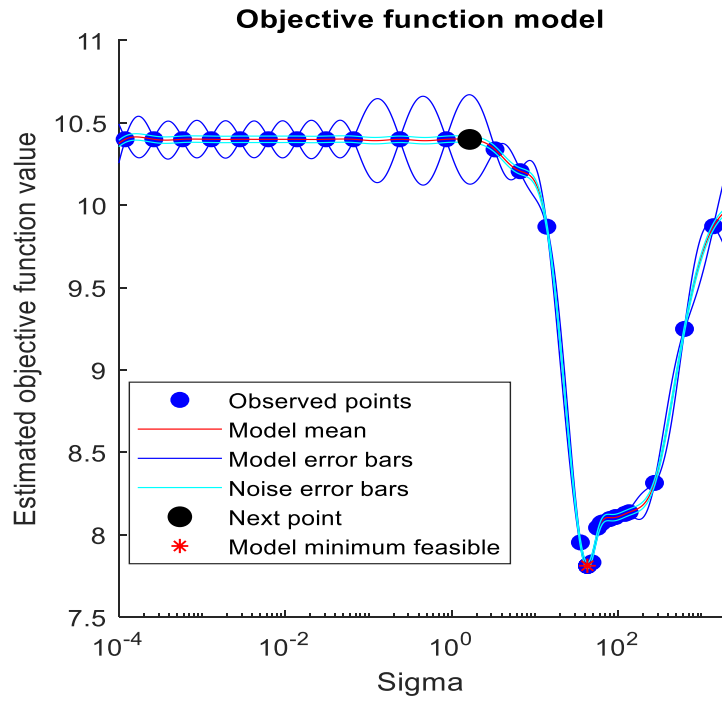


Fig. 13:: Objective function model after optimization

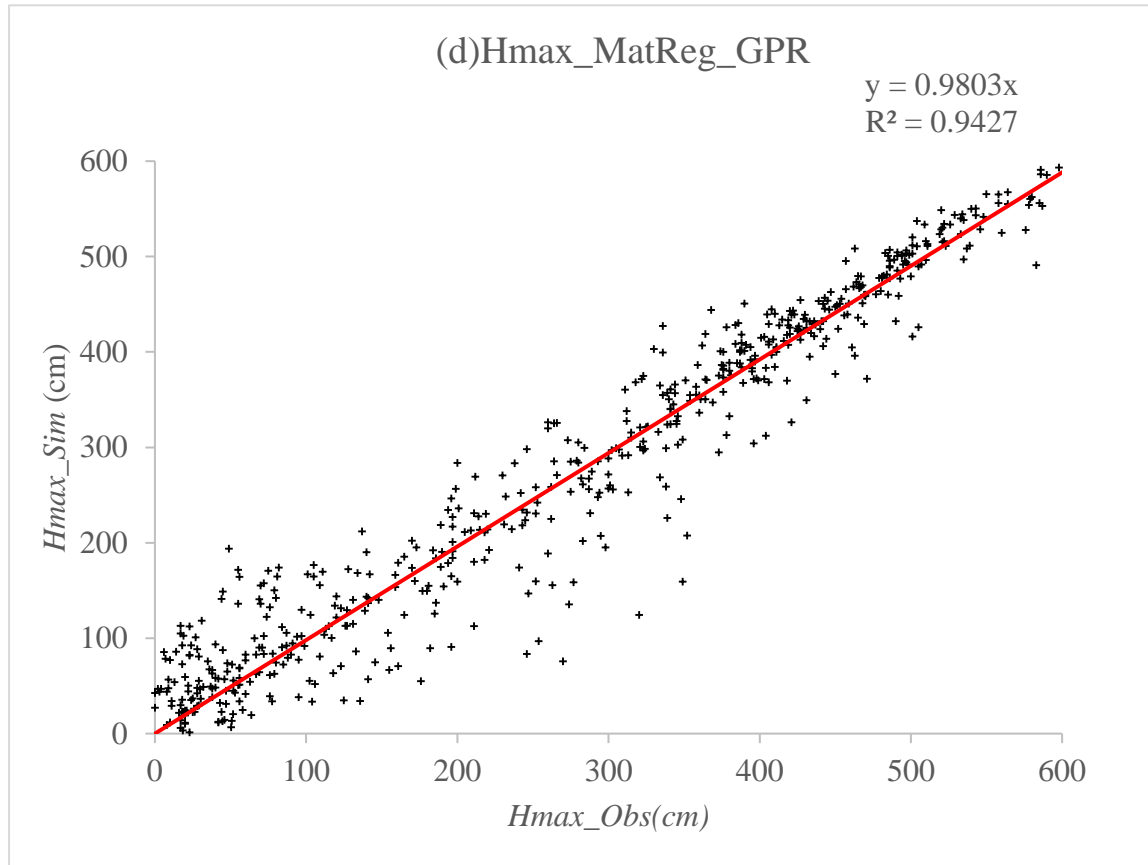


Fig. 14: Scatter plot of Observed versus Simulated WL Gaussian Process Regression (GPR)

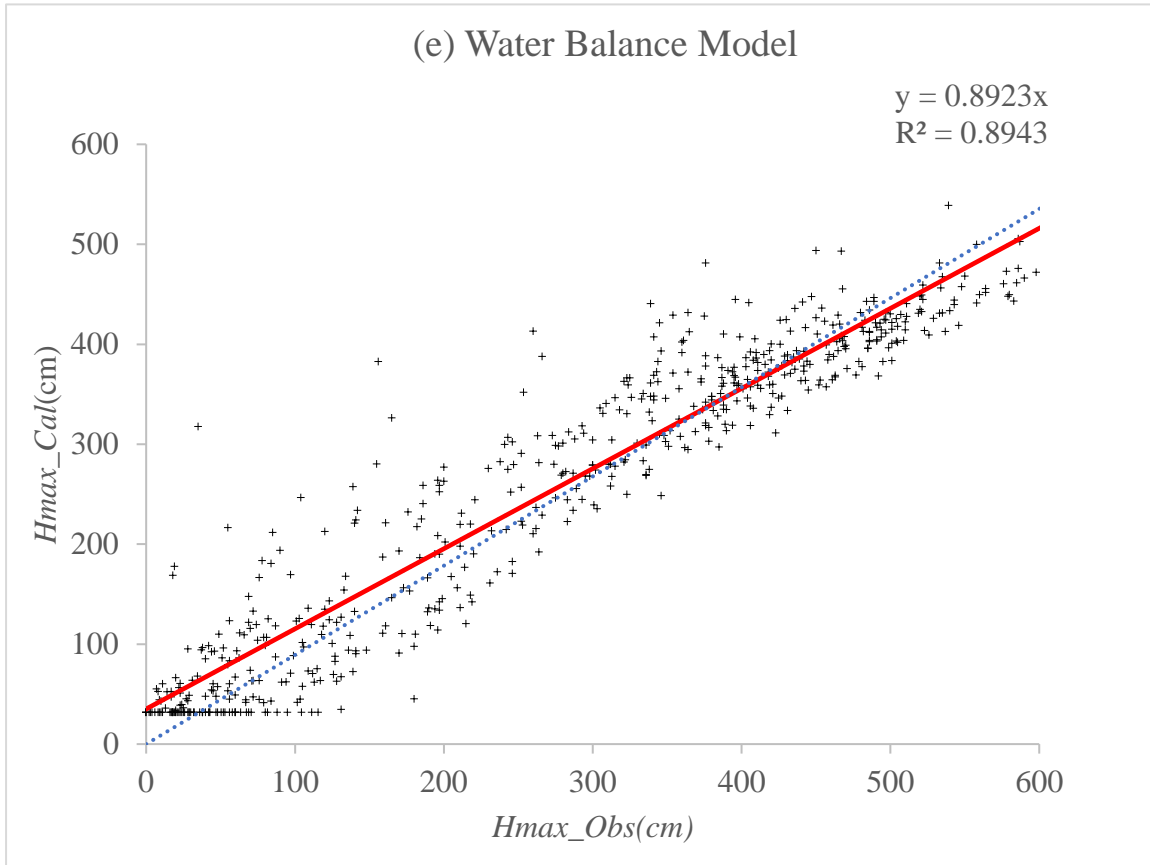


Fig. 15: Scatter plot of Observed versus Simulated WL Water Balance Model (WBM).

## **CHAPTER VI: DISCUSSION**

## 6.1. MODELS PERFORMANCE COMPARISON AFTER CALIBRATION

There is no single criterion which will play the role of a panacea in statistical model selection problems. Instead to use only the traditional criterion like RMSE, NSE and  $R^2$ , the Akaike Information Criterion (*AIC*), the Akaike Information Criterion corrected (*AICc*) and Bayesian Information Criterion (*BIC*) approaches were also used to evaluate each model (see 4.4.3.***Error! Reference source not found.***); these statistical criterions take account both the Sum Squared Error (*SSE*) and the number of parameters ( $p$ ) used for the model calibration (see eq. 23-25). The use of the Akaike Information Criterion corrected (*AICc*) for model selection is firmly based on a fundamental theory. When the number of parameters ( $p$ ) is large relative to sample size ( $n$ ) and should be used unless  $n/p > 40$  for the model with the largest value of  $p$  (Hurvich, et al., 1995). In this study we found that ANN LM\_1, ANN BR\_1, ANN BR\_2, ANN SCG\_1, GPR and WBM satisfied this condition. Therefore, the value of *AIC* for these models have been compute with the alternative formula (*AICc*).

By comparing only, the minimal values of each type of algorithm the results show clearly that the Levenberg-Marquardt has the minimal values for *AIC* (3297.65 with 15 hidden layers) and *BIC* (3411.42 with 3 hidden layers). Therefore, the *RMSE* for Bayesian Regularization (80 hidden layers) has the minimal value and slightly inferior to Levenberg -Marquardt' s *RMSE* with respectively 37.32 cm and 37.45 cm. The values of each criterion are shown in *Appendix 8* and *fig. 17-19* below.

From WBM we estimate during calibration process (data from 1960 to 2010) the monthly average variation of water body area ( $A_1 = 1,866 \sim 15,964 \text{ km}^2$ ) and wet area surrounding the water body ( $A_2 = 2,573 \sim 7,525 \text{ km}^2$ ) for a total flooded area size ( $A =$

4,438~23,480  $km^2$  ). The inflow fluctuated much more than the outflow due to the presence of several lakes in the delta; the monthly outflow varied significantly over a year  $Q_{out} = 54 \sim 1,859 m^3/s$  . The plot of comparison between the monthly measured incoming discharge  $Q_{in_{obs}}$  and simulated outgoing discharge  $Q_{out_{sim}}$  is shown in *fig 21*.

## 6.2. MODELS COMPARISON FOR PREDICTION

In order to compare the efficiency of each model for prediction, the dataset from 2011 to 2015 were chosen. The reference evapotranspiration, the rainfall and the flow were chosen like input data to compute the maximum monthly water-Level ( $H_{max}$ ). The performance indexes from the results of the different models (see *table 6*) indicate that the Artificial Neural Network with ANN Bayesian Regularization's algorithm has the minimal value of RMSE =40.24 cm follow by the Gaussian Process Regression with RMSE=40.56 cm and ANN Levenberg-Marquardt with RMSE=42.89 cm, also these models simulated water-level are the most correlated to the observed data and the maximum Nash-Sutcliffe Efficiency (NSE) as seen in *table 6*. As illustration, the plots of monthly Water-Level (WL) predicted with different models during the testing period (2011-2015) with the observed values of WL at Akka Station is shown in *fig 22*. Although, the WBM doesn't fit well as the other models for the water-level prediction for the validation period (see *fig. 15*), it allows to investigate some internal process occurring in the watershed.

The NID watershed behavior was evaluated with the Variable Source Area concept (Water Balance Model) in terms of variability of the inflow, the Rainfall-Runoff response and the change of wet soil surrounding the water body. The rainfall has few impacts on the delta, it represents only 13% of the total monthly average incoming water flow. The scatter plot of the water depth and the ratio of the areas size ( $A_2/A_1$ ) indicate that the water-level for the wet area to respond is 270 cm (2.7 m) as shown in *fig 20*.Fig..

Table 6: Performance indexes of different models during testing period (2011-2015)

	<i>Correl Coef ( r )</i>	<i>R<sup>2</sup></i>	<i>NSE</i>	<i>RMSE (cm)</i>
<i>Hmax_LM_15</i>	0.974	0.939	0.94	42.889
<i>Hmax_BR_80</i>	<b>0.975*</b>	<b>0.944*</b>	<b>0.95*</b>	<b>40.235*</b>
<i>Hmax_SCG_3</i>	0.961	0.934	0.91	45.426
<i>Hmax_Mat_GPR</i>	0.970	0.942	0.91	40.556
<i>Hmax_WBM</i>	0.964	0.904	0.84	50.801

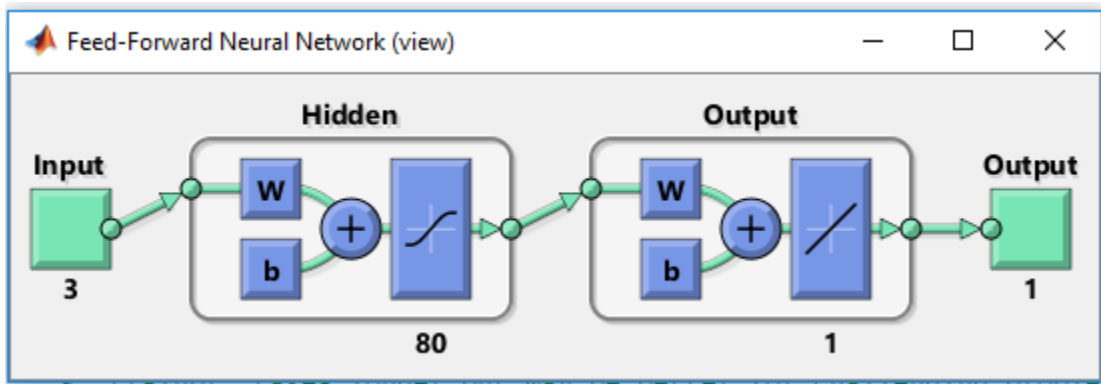


Fig. 16: Feed-Forward Neural Network Architecture for Bayesian Regularization

with 80 hidden layers

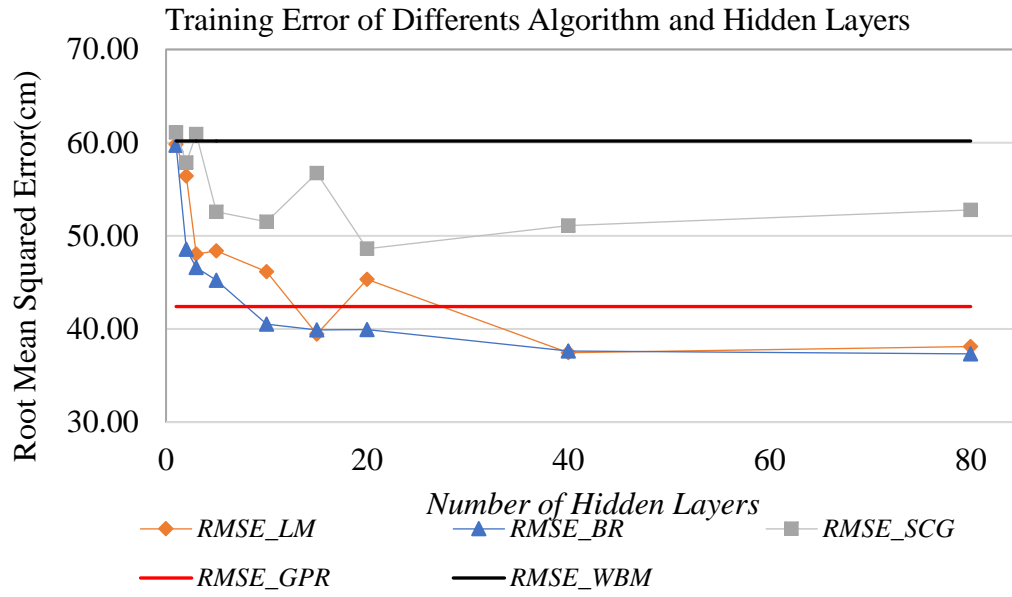


Fig.17: Root Mean Squared Error for differents models after calibration

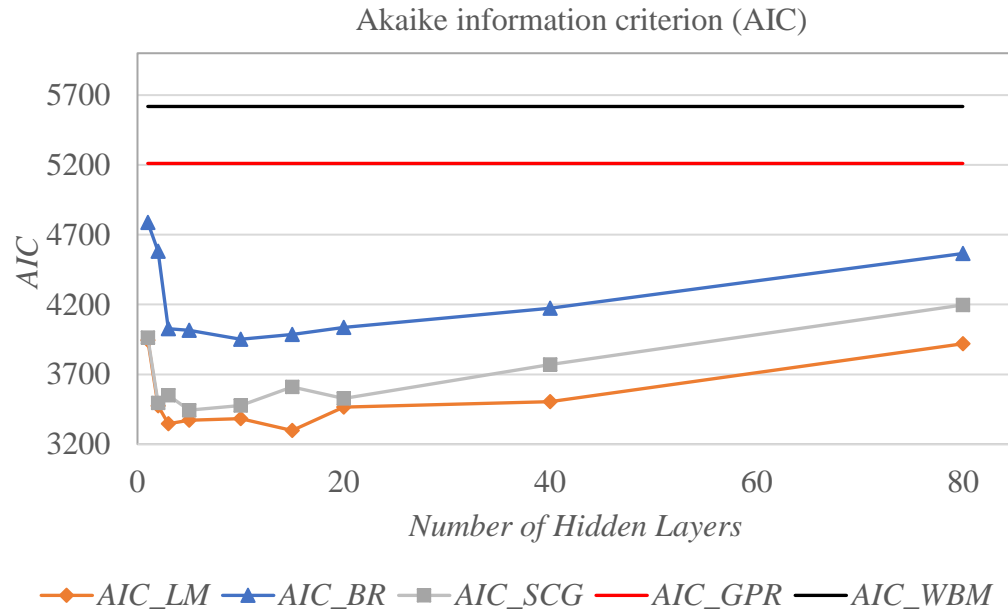


Fig. 18: Akaike Information Criterion for different models after calibration

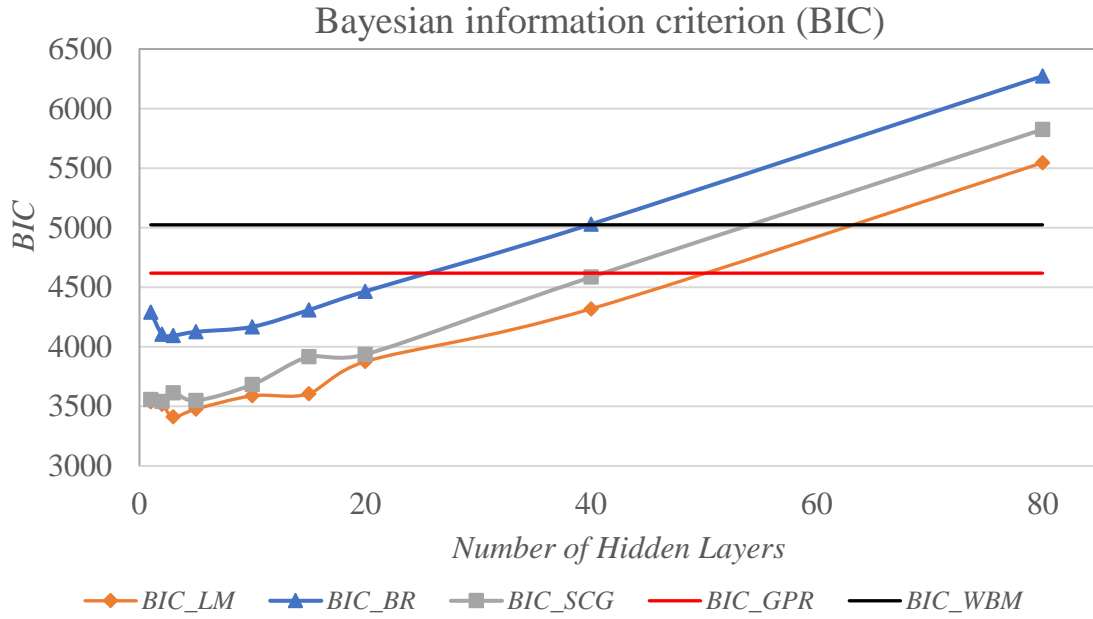


Fig.19: Bayesian Information Criterion for different models after calibration

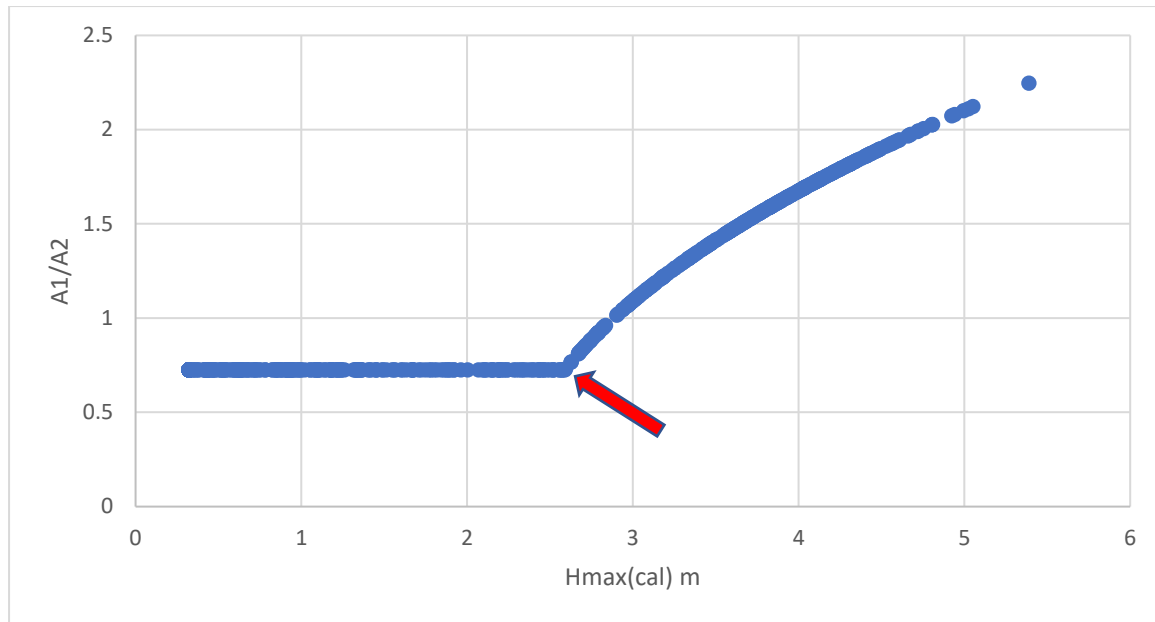


Fig.20: Relation of water depth H and area size ratio  $A_2/A_1$

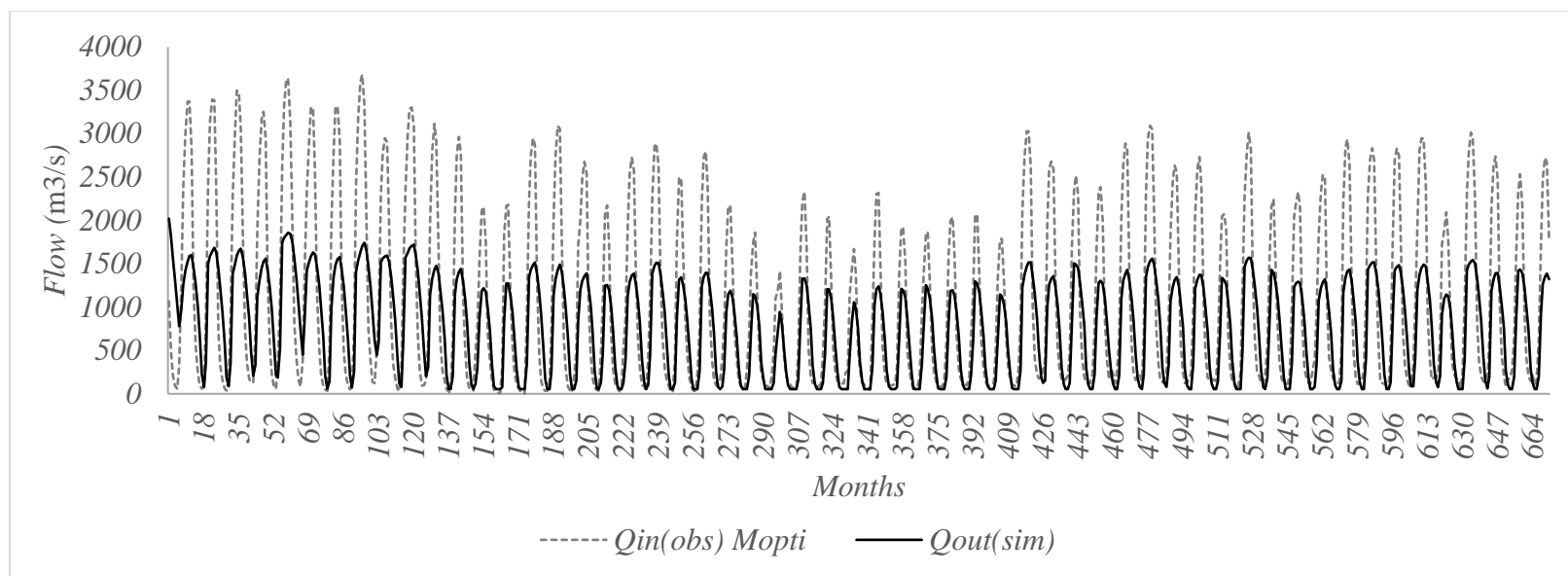


Fig.21: Comparison between the observed incoming discharge  $Q_{in(obs)}$  and simulated outgoing discharge  $Q_{out(sim)}$  from 1960 to 2010

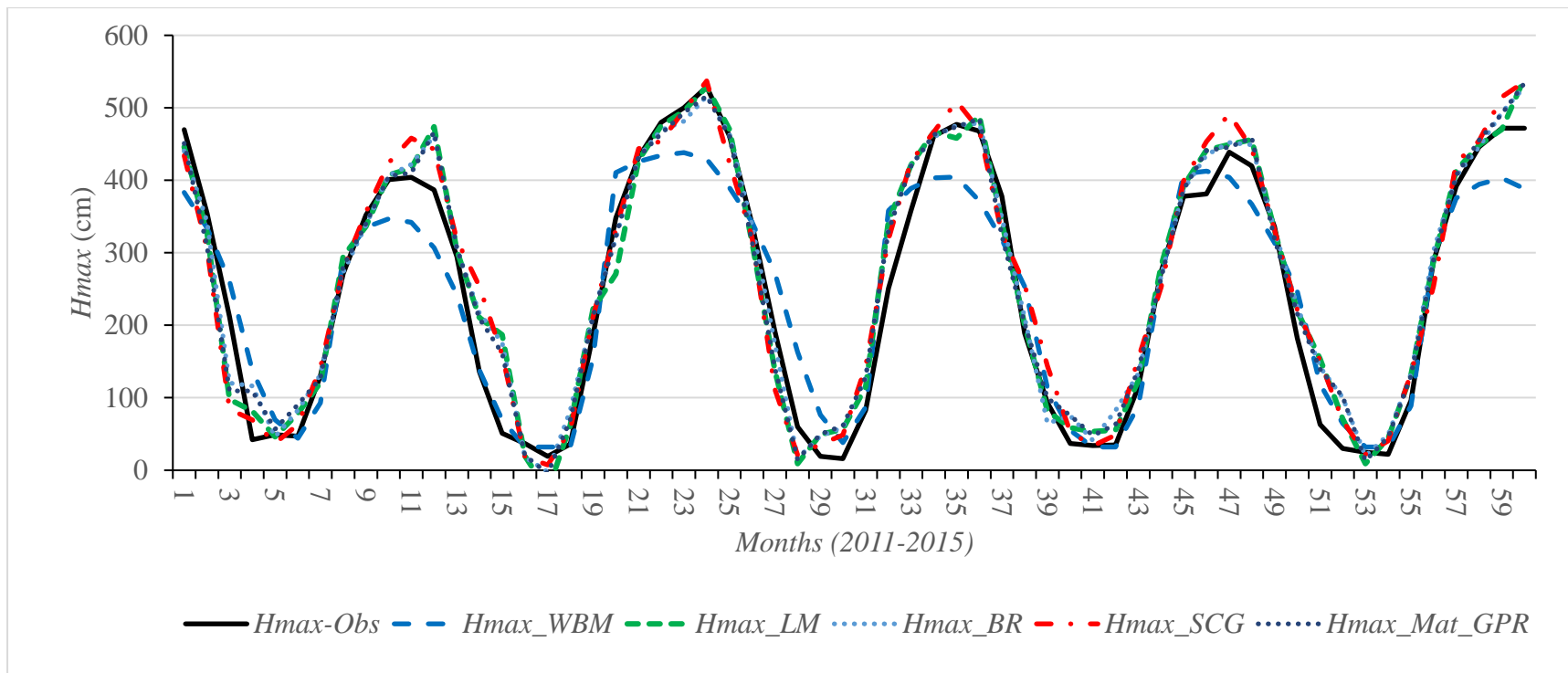


Fig. 22: Water-Level (WL) predicted with different models versus WL observed at Akka Station (2011-2015)

**CHAPTER VII: CONCLUSION AND SUMMARY**

## 6.1. CONCLUSIONS

The accuracy of different models for forecasting the maximum monthly water level of the Niger River Inner Delta was investigated using different statistical/stochastic methods with the input data of maximum monthly water inflow discharge ( $Q_{max}$ ) in Mopti station, the monthly Rainfall ( $R$ ) and Reference Evapotranspiration ( $ET_0$ ). From the results, the Artificial Neural Network (ANN) model with Bayesian Regularization algorithm has the minimal error to predict the water level of the Inner Niger Delta. However, the ANN Levenberg-Marquardt, the ANN Scaled Conjugate Gradient and the Gaussian Process Regression accuracies are close to ANN Bayesian Regularization.

Although, the ANN Bayesian Regularization gives the best fitting results, it doesn't allow to estimate all the internal process occurred in the watershed in opposite to the physically-based Water Balance Model using Variable Source Area. From WBM the wet area surrounding the water body of the delta ( $A_2 = 5,900 \sim 9,381 \text{ km}^2$ ) and the monthly outflow ( $Q_{out}$ ) were estimate. The inflow fluctuated much more than the outflow due to the presence of several lakes in the delta.

Owing the lack of climate data throughout the large area of the NID with  $40,000 \text{ km}^2$  (only one station), the WBM couldn't compute accurately, therefore the ANN is a best alternative to overcome this issue.

After the major droughts in the 1970s and 1980s, rainfall in the Inner Delta region has improved over the last decade. This condition, however, remains fragile as it has been impacted by climate

change and the rapid expansion of dams' construction and irrigation. The use of the new IT technology of Artificial Intelligence to develop an accurate hydrological model to forecast the seasonal and inter-annual Water-Level in the NID could be good tool for engineers and policymakers in order to make a balance between development project (irrigation, hydropower, etc..) and the sustainability of the NID wetland on which millions of people and wildlife depends.

## 6.2. SUMMARY

The aim of this graduation thesis *Hydrological Modelling for the Conservation of the Niger Inner Delta in Mali* is to test different approaches for forecasting the Water-Level of the Niger Inner Delta (NID). This delta is the third biggest wetland under RAMSAR convention and constitute a habitat for various biodiversity and a livelihood for millions of people through fishery, farming, animal breeding etc..... The traditional Water Balance Models for hydrological forecasting required many input data and some of those data are missing or difficult to get in the area of NID like groundwater, water withdrawal flows for agriculture and urban life, soils feature for infiltration etc... To overcome these issues, alternatives ways of hydrological modelling were investigated: Artificial Neural Network (ANN), Gaussian Process Regression (GPR) statistical model and Water Balance Model (WBM) using Variable Source Area concept.

...In this study we were able to:

1. Understand the context of the study area, not only in term of scientific prospective, but also in term of socio-economic situation through litterature reviews and our own experiences in-situ;
2. Collect and prepare the data from different sources (assessed its condition including looking for the trends, outliers, exceptions, incorrect, inconsistent) for the hydrological modelling.
3. Develop and calibrate differents type of hydrology models from the most physical based Water Balance Model to the most stochastic Artificial Neural Network in order to forecast the Water-Level of the Niger Inner Delta.
4. Compare and test the develop hydrological models based on differents evaluation criterions like RMSE, NSE, AIC, AICc and BIC.

From the results:

1. The ANN model with Bayesian Regularization algorithm has the minimal error to predict the water level of the Inner Niger Delta. However, the ANN Levenberg-Marquardt, the ANN Scaled Conjugate Gradient and the Gaussian Process Regression accuracies are close to ANN Bayesian Regularization.
2. Although, the ANN Bayesian Regularization gives the best fitting results, it doesn't allow to estimate all the internal process occurred in the watershed in opposite to the physically-based Water Balance Model using Variable Source Area. From WBM the wet area surrounding the water body of the delta ( $A_2 = 5,900 \sim 9,381 \text{ km}^2$ ) and the monthly outflow ( $Q_{out}$ ) were estimate
3. Owing the lack of climate data throughout the large area of the NID with 40,000 km<sup>2</sup> (only one station), the WBM couldn't forecast accurately its the Water-Level, therefore the ANN is a good alternative to overcome this issue.

The use of the new IT technology of Artificial Intelligence to develop an accurate hydrological model to forecast the seasonal and inter-annual Water-Level in the NID could be a good tool for engineers and policymakers in order to make a balance between development project (irrigation, hydropower, etc..) and the sustainability of the NID wetland on which millions of people and species depends.

---

**REFERENCES**

- Adama CESSOUMA** Agriculture Irrigee et les Perspectives Economies d'Eau au Mali [Journal] // International Journal of Revue HTE. -. - Vol. 141. - pp. 125-131, 2008.
- Agarwal Anil [et al.]** Integrated Water Management [Report]. - Stockholm : Global Water Partnership, 2000.
- Akaike Hirotogu** Fitting Autoregressive Models for Prediction [Journal] // Annals of the Institute of Statistical Mathematics. -. - 1 : Vol. 21. - pp. 243-247, 1969.
- Akaike Hirotugu** A New Look at the Statistical Model Identification [Journal] // IEEE Transaction on Automatic Control. -. - 6 : Vols. ac-19. - pp. 716-723, 1974.
- Andersen Inger [et al.]** The Niger River Basin: A Vision of Sustainable Management [Report]. - Washington,DC : THE WORLD BANK, 2005.
- Beale Mark Hudson, Hagan Martin T. and Demuth Howard B.** MatLab Neural Network Toolbox TM User Guide [Book]. - Natick : Mathworks Inc., - Vol. R2018, 2018.
- Betson Roger P.** What is Watershed Runoff [Journal] // Journal of Geophysical Research. -. - 8 : Vol. 69. - pp. 1541-1552, 1964.
- Cisse Modibo Galy** Conflits sociaux, mobilité interne et externe des sociétés riveraines du fleuve Niger des communes de Djenné, du Kéwa et du Pondori [Report]. - Bamako : Universite de Bamako, Centre de Recherche en Anthropologie de l'Eau, 2009.
- Curry B. and Morgan P. H.** Model Selection in Neural Networks: Somme Difficulties [Journal] // European Journal of Operational Research. -. - 2 : Vol. 170. - pp. 567-577, 2006.
- Dawson C.W. and Wilby R.L.** Hydrological modelling using Artificial Neural Networks [Journal] // Progress in Physical Geography. -. - 1 : Vol. 25. - pp. 80-108, 2001.
- Dawson Christian W. and Wilby Robert** An artificial neural network approach to rainfall-runoff modelling [Journal] // Hydrological Sciences Journal. -. - 1 : Vol. 43. - pp. 47-66, 2009.
- Dooge J.C. I.** The Development of Hydrological Concepts in Britain and Ireland between 1674 and 1874 [Journal] // Hydrological Sciences Journal. -. - 3 : Vol. 19. - pp. 279-302, 1974.
- Dunne Thomas and Black Richard D.** Partial area contributions to Storm Runoff in a small New England Watershed [Journal] // Water Resources research. -. - 5 : Vol. 6. - pp. 1296-1311, 1970.
- Dunne Thomas, Moore T. R. and Taylor C. H.** Recognition and Prediction of Runoff-Producing Zones in Humid Regions [Journal] // Hydrological Science. -. - 3 : Vol. XX. - pp. 305-325, 1975.
- Engman Edwin T. and Rogowski Andrew S.** A partial Area Model for Storm Flow Synthesis [Journal] // Water Resources Research. -. - 3 : Vol. 10. - pp. 464-472, 1974.

- FAO W.W.C.** Towards a Water and Food Secure Future, Critical Perspectives for Policy-Makers [Report]. - Marseille : FAO, 2015.
- Foresee F. Dan and Hagan Martin T.** Gauss-Newton Approximation to Bayesian Learning [Conference] // International Conference on Neural Network. - Houston, TX, USA : [s.n.], 1997.
- Fortier General** Africa on Web [Online]. -. - www.africa-onweb.com, 1915.
- Gallais Jean** Le Delta intérieur du Niger : étude de géographie régionale [Book]. - Dakar : I.F.A.N. ASIN: B0014W6XFO, 1967.
- Garrett Hardin** The Tragedy of the Commons [Journal] // American Association for the Advancement of Science. -. - 3859 : Vol. 162. - pp. 1243-1248, 1968.
- Govindaraju Rao S.** Artificial Neural Networks in hydrology. II: Hydrologic applications [Journal] // Journal of Hydrologic Engineering. -. - 2 : Vol. 5. - pp. 124-137, 2000.
- Govindaraju Rao S.** Artificial neural networks in hydrology. I: Preliminary concepts [Journal] // Journal of Hydrologic Engineering. -. - 2 : Vol. 5. - pp. 115-123, 2000.
- Halley Edmond** An Estimate of the Quantity of Vapour Raised out of the Sea by the Warmth of the Sun [Journal] // Philosophical Transactions. -. - 1 : Vol. 16. - pp. 366-370, 1686.
- Hewlett John D. and Hibbert Alden R.** Factors affecting the response of small watersheds to precipitation in humid areas [Journal] // Progress in Physical Geography. -. - 2 : Vol. 33. - pp. 288–293, 1967.
- Horton Robert E.** Role of Infiltration in Hydrologic Cycle [Journal] // Transaction American Geophysical Union. - New York : [s.n.],. - 1 : Vol. 26. - pp. 446-460, 1933.
- Hurvich Clifford M. and Tsai Chin-Ling** Model Selection for Extended Quasi-Likelihood Models in Small Samples [Journal] // BIOMETRIC. -. - 3 : Vol. 51. - pp. 1077-1084, 1995.
- Ibrahim Moussa [et al.]** Water Balance Analysis over the Niger Inland Delta-Mali: Spatio-temporal Dynamics of the Flood Area Water Losses [Journal] // MDPI-HYDROLOGY. -. - 40 : Vol. 4. - pp. 1-23, 2017.
- INSTAT-MALI** Modular and Permanent Survey of Households (MPSH) First Report [Report]. - Bamako : INSTAT, 2016.
- Int. Crisis Group** Central Mali: An Uprising in the Making? [Report]. - Brussels : International Crisis Group, 2016.
- Kassambara Barry, Ganji Homayoon and Takamitsu Kajisa** Impact of Agriculture Water Allocation on the Ecosystems in the Inner Niger River Delta [Journal] // International Journal of GEOMATE. - Japan : International Journal of GEOMATE,. - 42 : Vol. 14. - pp. 164-170, 2018.

- Khan Mohammad Sajjad and Coulibaly Paulin** Application of Support Vector Machine in Lake Water Level Prediction [Journal] // Journal of Hydrology Engineering. -. - Vol. 11. - pp. 199-205, 2006.
- Kuper Marcel [et al.]** Integrated modelling of the ecosystem of the Niger river inland delta in Mali [Journal] // Ecological Modelling. -. - 1 : Vol. 164. - pp. 83-102, 2003.
- Kusterer John M. [et al.]** Atmospheric Science Data Center [Online]. - NASA. - 10 26,. - <https://earthdata.nasa.gov>, 2018.
- Lee M. T. and Delleur J. W.** A Variable Source Area Model of Rainfall-Runoff Process Based on the Watershed Stream Network [Journal] // Water Resources Research. -. - 5 : Vol. 12. - pp. 1029-1036, 1976.
- Lemly Dennis A, Kingsford Richard T. and Thompson Julian R.** Irrigated Agriculture and Wildlife Conservation: Conflict on a Global Scale [Journal] // International Journal of Environment Management. -. - 5 : Vol. 25. - pp. 485-512, 2000.
- Li Jin Yan and Chow T. W S** Estimation theory and optimization algorithm for the number of hidden units in the higher-order feedforward neural network [Conference] // IEEE International Conference on Neural Networks. - Perth, Aust : [s.n.], 1995.
- LLoyd William Forster** Two lectures on the checks to population : delivered before the University of Oxford, in Michaelmas term [Book]. - Oxford : Oxford University Press, 1833.
- MacKay David J. C.** Bayesian Interpolation [Journal] // Computation and Neural Systems. -. - Vol. 4. - pp. 415-447, 1992.
- Mahe Gil [et al.]** Water losses in the inner delta of the River Niger: water balance and flooded area [Journal] // Hydrological Processes. -. - 22 : Vol. 23. - pp. 3157-3160, 2009.
- Marieu B. [et al.]** Actualisation des donnees hydrometriques du fleuve niger au Mali pour EQUANIS [Report]. - Bamako : Programme PEGI/GBF/EQUANIS, 1998.
- Marquardt Donald W.** An Algorithm for Least-Squares Estimation of Nonlinear Parameters [Journal] // J. Soc. INDUST. APPL. MATH.. -. - 2 : Vol. 11. - pp. 431-441, 1963.
- MohammadKalteh Aman** Monthly riverflow forecasting using artificial neural network and support vector regression models coupled with wavelet transform [Journal] // ELSEVIER. -. - Vol. 54. - pp. 1-8, 2013.
- Moller Martin Dodslette** A Scaled Conjugate Gradient Algorithm for Fast Supervised Learning [Journal] // Neural Networks. -. - Vol. 6. - pp. 525-533, 1993.
- Moriasi Daniel N. [et al.]** Model Evaluation Guidelines for Systematic Quantification of accuracy in Watershed Simulations [Journal] // ASABE Soil & Water Division. -. - 3 : Vol. 50. - pp. 885-900, 2007.

- Moyal J E** Causality, Determinism and Probability [Journal] // Philosophy. -. - 91 : Vol. 24. - pp. 310-317, 1949.
- Mulvany Thomas J.** On the use of self-registering rain and flood gauges in making observations of the relations of rain fall and flood discharges in a given catchment. [Journal] // Transactions of the Institution of Civil Engineers of Ireland. -. - 2 : Vol. 4. - pp. 18-33, 1851.
- Naghetini Mauro** Fundamentals of Statistical Hydrology [Book]. - Belo Horizonte, Brazil : Springer, 2016.
- Ogilvie Andrew [et al.]** Decadal monitoring of the Niger Inner Delta flood dynamics using MODIS optical data [Journal] // Journal of Hydrology. -. - 523 : Vol. 1. - pp. 368-383, 2015.
- Orange Didier [et al.]** Hydrologie, agro-écologie et superficies d'inondation dans le delta intérieur du fleuve Niger [Journal] // Gestion Intégrée des Ressources Naturelles en Zones Inondables Tropicales. - Bamako : [s.n.],. - pp. 208-228, 2002.
- Özgür Kişi** Streamflow Forecasting Using Different Artificial Neural Network Algorithms [Journal] // JOURNAL OF HYDROLOGIC ENGINEERING. -. - 5 : Vol. 12. - pp. 532-539, 2007.
- Programme United Nations Development** Human Development Report 2015 (Work for human development) [Report]. - New York : UNDP, 2015.
- Ramsar** Fact Sheet: Inner Niger Delta/Delta Interieur du fleuve Niger (Mali) [Report]. - Gland : Ramsar, 2004.
- Rasmussen Carl Edward and Williams Christopher K. I.** Gaussian Processes for Machine Learning [Book]. - Cambridge, Massachusetts : The MIT Press, 2006.
- Rezaeianzadeh M [et al.]** Flood flow forecasting using ANN, ANFIS and regression models [Journal] // Springer. -. - 1 : Vol. 25. - pp. 25-37, 2014.
- Rezaeianzadeh M., Tabari H. and Arabi Yazdi A.** Flood flow forecasting using ANN, ANFIS and regression models [Journal] // Springer-Verlag. -. - 1 : Vol. 25. - pp. 25-37, 2014.
- Risley John C. [et al.]** An Analysis of Statistical Methods for Seasonal Flow Forecasting in the Upper Klamath River Basin of Oregon and California [Book]. - Reston, Virginia : U.S. Geological Survey (USGS), 2005.
- Rosenberg Eric A., WOOD Andrew W. and STEINEMANN Anne C.** Statistical applications of physically based hydrologic models to seasonal streamflow forecasts [Journal] // WATER RESOURCES RESEARCH. -. - W00H14 : Vol. 47. - pp. 1-19, 2011.
- Schwarz Gideon** Estimating the Dimension of a Model [Journal] // The Annals of Statistics. -. - 2 : Vol. 6. - pp. 461-464, 1978.
- Sheela K. Gnana and Deepa S. N.** Review on Methods to Fix Number of Hidden Neurons in Neural Networks [Journal] // Hindawi. -. - 1 : Vol. 2013. - pp. 1-11, 2013.

**Simonoff Jeffrey S.** Smoothing Methods in Statistics [Book]. - New York : Springer Series in Statistics, 1998.

**Tamura S. and Tateishi M.** Capabilities of a four-layered feedforward neural network: four layers versus three [Journal] // IEEE Transactions on Neural Networks. -. - 2 : Vol. 8. - pp. 251-255, 1997.

**Torres Jordi** Towards Data Science [Online]. - UPC Barcelona Tech & Barcelona Supercomputing Center, September 21, 2018. - 12 10,. - <https://towardsdatascience.com/how-do-artificial-neural-networks-learn773e46399fc7>, 2018.

**Warburton-Lee John and Pavitt Nigel** Alamy [Online]. - [www.alamyimages.fr](http://www.alamyimages.fr).

**Wolock David M.** Simulating the Variable-Source-Area Concept of Streamflow Generation with the Watershed Model TOPMODEL [Report]. - Lawrence, Kansas : U.S. Geological Survey, 1993.

**Xiong Lihua, O'Connor Kieran M. and Guo Shenglian** Comparison of three Updating Schemes Using Artificial Neural Network in Flow Forecasting [Journal] // Hydrology and Earth System Sciences. -. - 2 : Vol. 8. - pp. 247-255, 2004.

**Yu Zhen [et al.]** ARIMA Modelling and Forecasting of Water Level in the Middle Reach of the Yangtze River [Conference] // ICTIS. - Banff(CANADA) : [s.n.]. - pp. 172-177, 2017.

**Zadeh Mehdi Rezaeian [et al.]** Daily Outflow Prediction by Multi Layer Perceptron with Logistic Sigmoid and Tangent Sigmoid Activation Functions [Journal] // Springer. -. - 1 : Vol. 24. - pp. 2673–2688, 2010.

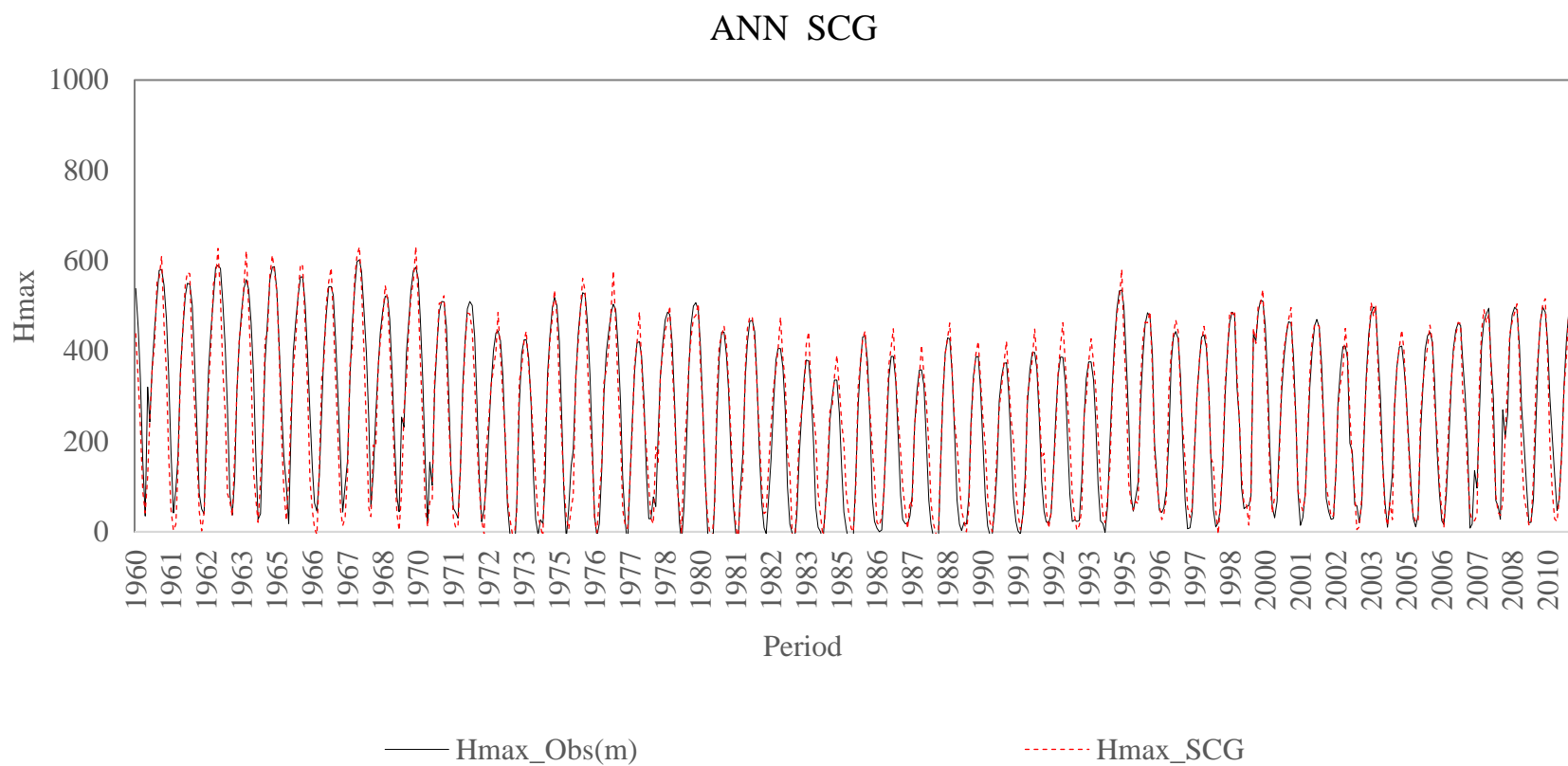
**Zwarts Leo [et al.]** The Niger, a lifeline Effective water management in the Upper Niger Basin [Report]. - Bamako : Wetland International, 2005.

**APPENDIX**

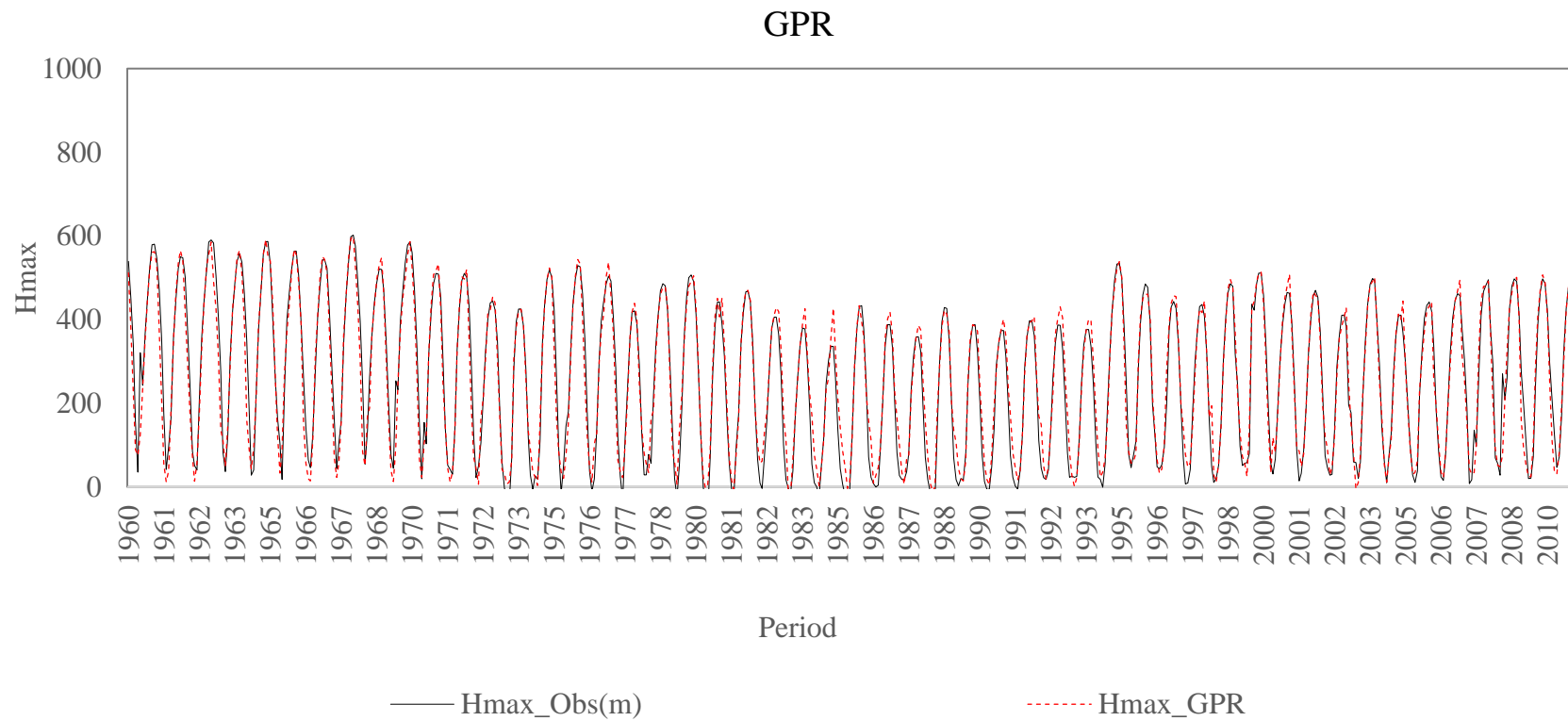




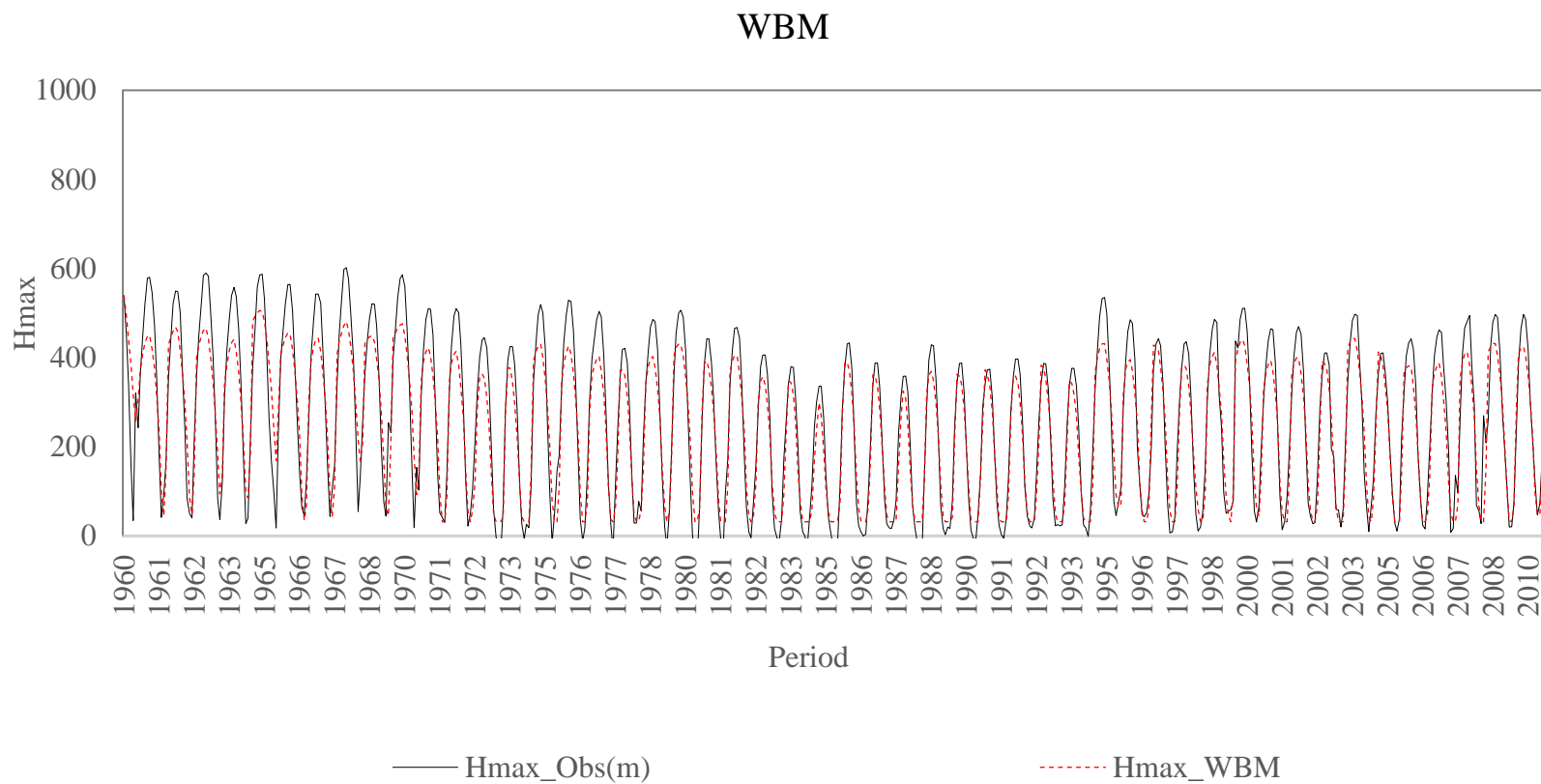
**Appendix 3:** plots of Observed Maximum Water-Level (Hmax\_Obs) VS Calculated Maximum Water-Level with Scaled Conjugate Gradient (Hmax\_SCG)



**Appendix 4:** plots of Observed Maximum Water-Level (Hmax\_Obs) VS Calculated Maximum Water-Level with Gaussian Process Regression (Hmax\_GPR)



**Appendix 5:** plots of Observed Maximum Water-Level (Hmax\_Obs) VS Calculated Maximum Water-Level with Water Balance Model using Variable Source Area(Hmax\_WBM)



## Appendix 6: Autoregression Problem with External Input with a NARX Neural Network Script for Bayesian Regularization feedforward

```

% This script assumes these variables are defined:
%
% NN_Input - input time series.
% NN_Target - feedback time series.

X = tonndata(NN_Input,true,false);
T = tonndata(NN_Target,true,false);

% Choose a Training Function
% For a list of all training functions type: help ntrain
% 'trainlm' is usually fastest.
% 'trainbr' takes longer but may be better for challenging problems.
% 'trainscg' uses less memory. Suitable in low memory situations.
trainFcn = ' trainbr '; % Bayesian Regularization backpropagation.

% Create a Nonlinear Autoregressive Network with External Input
inputDelays = 1:2;
feedbackDelays = 1:2;
hiddenLayerSize = 80;
net = narxnet(inputDelays,feedbackDelays,hiddenLayerSize,'open',trainFcn);

% Choose Input and Feedback Pre/Post-Processing Functions
% Settings for feedback input are automatically applied to feedback output
% For a list of all processing functions type: help nprocess
% Customize input parameters at: net.inputs{i}.processParam
% Customize output parameters at: net.outputs{i}.processParam
net.inputs{1}.processFcns = {'removeconstantrows','mapminmax'};
net.inputs{2}.processFcns = {'removeconstantrows','mapminmax'};

% Prepare the Data for Training and Simulation
% The function PREPARETS prepares timeseries data for a particular network,
% shifting time by the minimum amount to fill input states and layer
% states. Using PREPARETS allows you to keep your original time series data
% unchanged, while easily customizing it for networks with differing
% numbers of delays, with open loop or closed loop feedback modes.
[x,xi,ai,t] = preparets(net,X,{},T);

% Setup Division of Data for Training, Validation, Testing
% For a list of all data division functions type: help nndivision
net.divideFcn = 'dividerand'; % Divide data randomly
net.divideMode = 'time'; % Divide up every sample
net.divideParam.trainRatio = 70/100;
net.divideParam.valRatio = 15/100;
net.divideParam.testRatio = 15/100;

% Choose a Performance Function
% For a list of all performance functions type: help nnperformance
net.performFcn = 'mse'; % Mean Squared Error

% Choose Plot Functions
% For a list of all plot functions type: help nnplot

```

---

```

net.plotFcns = {'plotperform','plottrainstate','ploterrhist', ...
    'plotregression','plotresponse','ploterrcorr','plotinerrcorr'};

% Train the Network
[net,tr] = train(net,x,t,xi,ai);

% Test the Network
y = net(x,xi,ai);
e = gsubtract(t,y);
performance = perform(net,t,y)

% Recalculate Training, Validation and Test Performance
trainTargets = gmultiply(t,tr.trainMask);
valTargets = gmultiply(t,tr.valMask);
testTargets = gmultiply(t,tr.testMask);
trainPerformance = perform(net,trainTargets,y)
valPerformance = perform(net,valTargets,y)
testPerformance = perform(net,testTargets,y)

% View the Network
view(net)

% Plots
% Uncomment these lines to enable various plots.
%figure, plotperform(tr)
%figure, plottrainstate(tr)
%figure, ploterrhist(e)
%figure, plotregression(t,y)
%figure, plotresponse(t,y)
%figure, ploterrcorr(e)
%figure, plotinerrcorr(x,e)

% Closed Loop Network
% Use this network to do multi-step prediction.
% The function CLOSELOOP replaces the feedback input with a direct
% connection from the outout layer.
netc = closeloop(net);
netc.name = [net.name ' - Closed Loop'];
view(netc)
[xc,xic,aic,tc] = preparets(netc,X,{},T);
yc = netc(xc,xic,aic);
closedLoopPerformance = perform(net,tc,yc)

% Multi-step Prediction
% Sometimes it is useful to simulate a network in open-loop form for as
% long as there is known output data, and then switch to closed-loop form
% to perform multistep prediction while providing only the external input.
% Here all but 5 timesteps of the input series and target series are used
% to simulate the network in open-loop form, taking advantage of the higher
% accuracy that providing the target series produces:
numTimesteps = size(x,2);
knownOutputTimesteps = 1:(numTimesteps-5);
predictOutputTimesteps = (numTimesteps-4):numTimesteps;
X1 = X(:,knownOutputTimesteps);
T1 = T(:,knownOutputTimesteps);

```

```

[x1,xio,aio] = preparets(net,X1,{},T1);
[y1,xfo,afo] = net(x1,xio,aio);
% Next the the network and its final states will be converted to
% closed-loop form to make five predictions with only the five inputs
% provided.
x2 = X(1,predictOutputTimesteps);
[netc,xic,aic] = closeloop(net,xfo,afo);
[y2,xfc,afc] = netc(x2,xic,aic);
multiStepPerformance = perform(net,T(1,predictOutputTimesteps),y2)
% Alternate predictions can be made for different values of x2, or further
% predictions can be made by continuing simulation with additional external
% inputs and the last closed-loop states xfc and afc.

% Step-Ahead Prediction Network
% For some applications it helps to get the prediction a timestep early.
% The original network returns predicted y(t+1) at the same time it is
% given y(t+1). For some applications such as decision making, it would
% help to have predicted y(t+1) once y(t) is available, but before the
% actual y(t+1) occurs. The network can be made to return its output a
% timestep early by removing one delay so that its minimal tap delay is now
% 0 instead of 1. The new network returns the same outputs as the original
% network, but outputs are shifted left one timestep.
nets = removedelay(net);
nets.name = [net.name ' - Predict One Step Ahead'];
view(nets)
[xs,xis,ais,ts] = preparets(nets,X,{},T);
ys = nets(xs,xis,ais);
stepAheadPerformance = perform(nets,ts,ys)

% Deployment
% Change the (false) values to (true) to enable the following code blocks.
% See the help for each generation function for more information.
if (false)
    % Generate MATLAB function for neural network for application
    % deployment in MATLAB scripts or with MATLAB Compiler and Builder
    % tools, or simply to examine the calculations your trained neural
    % network performs.
    genFunction(net,'myNeuralNetworkFunction');
    y = myNeuralNetworkFunction(x,xi,ai);
end
if (false)
    % Generate a matrix-only MATLAB function for neural network code
    % generation with MATLAB Coder tools.
    genFunction(net,'myNeuralNetworkFunction','MatrixOnly','yes');
    x1 = cell2mat(x(1,:));
    x2 = cell2mat(x(2,:));
    xi1 = cell2mat(xi(1,:));
    xi2 = cell2mat(xi(2,:));
    y = myNeuralNetworkFunction(x1,x2,xi1,xi2);
end
if (false)
    % Generate a Simulink diagram for simulation or deployment with.
    % Simulink Coder tools.
    gensim(net);
end

```

**Appendix 7: Parameters of the Bayesian Regularization Neural Networks with 80 hidden layers**

Weights				Biases
$IW_{ij}$			$LW_i$	$b$
-0.0115	-0.0516	-0.0451	0.22205	-0.20438
0.96608	-1.8754	-1.505	-2.2321	-2.760043
0.01079	0.0486	0.04333	-0.2062	0.190028
0.00384	0.0176	0.01824	-0.0717	0.0667605
0.01103	0.04968	0.04396	-0.2116	0.1949755
0.01103	0.04967	0.04396	-0.2116	0.1949295
-0.0089	-0.0401	-0.0377	0.16624	-0.153744
-0.0111	-0.05	-0.0441	0.21318	-0.196367
-0.0115	-0.0519	-0.0452	0.22333	-0.205538
-1.7861	-2.4364	2.00897	-1.1331	1.0332717
0.01123	0.05059	0.04448	-0.2164	0.1992475
0.01133	0.05103	0.04473	-0.2187	0.2013653
-0.9837	0.94616	-0.7147	-1.7216	0.8395833
-3.1889	0.83658	-1.5709	-0.7222	0.2396011
-0.0109	-0.0493	-0.0437	0.2095	-0.193033
-0.011	-0.0496	-0.0439	0.21149	-0.194838
-0.2937	0.21215	-2.9537	-2.5355	-2.820479
0.01095	0.04932	0.04375	-0.2098	0.1933394
0.01107	0.04984	0.04406	-0.2125	0.1957331
-0.0107	-0.0481	-0.043	0.20387	-0.187942
-0.0085	-0.0384	-0.0365	0.15901	-0.147144
0.01135	0.05113	0.04479	-0.2193	0.201862
-0.0108	-0.0488	-0.0435	0.20722	-0.190973
-0.0116	-0.0525	-0.0455	0.22648	-0.208381
-0.012	-0.0544	-0.0465	0.23783	-0.218622
-0.0111	-0.05	-0.0442	0.21341	-0.196577
-0.0076	-0.0346	-0.0335	0.14243	-0.131974
0.00999	0.04502	0.04108	-0.1888	0.1742405
0.01084	0.04883	0.04347	-0.2074	0.1910902
0.01094	0.04928	0.04373	-0.2096	0.1931331
0.0104	0.04686	0.04226	-0.1976	0.1822416
-0.0105	-0.0472	-0.0425	0.19922	-0.183724
-0.9198	-0.2339	-1.7895	1.45315	-1.577963
0.41175	-1.7875	1.41139	-0.895	-0.93071
0.01096	0.04934	0.04377	-0.2099	0.1934361
-0.0023	-0.0107	-0.0112	0.04351	-0.040533
-0.0105	-0.0475	-0.0426	0.2006	-0.18498
0.53119	-1.1518	-3.7332	1.70934	-3.886972
-0.0106	-0.0478	-0.0429	0.20233	-0.186546
-0.0015	-0.0069	-0.0073	0.02813	-0.026214
1.42796	-0.2078	-1.6482	1.06555	-0.844971
0.01022	0.04604	0.04174	-0.1936	0.178638
-1.6486	0.45556	-0.5669	1.74352	-0.387602

Weights				Biases
IW <sub>ij</sub>			LW <sub>i</sub>	b
-0.0047	-0.0216	-0.0221	0.08821	-0.082022
0.01119	0.05041	0.04438	-0.2155	0.1984383
0.01146	0.05162	0.04506	-0.2219	0.2042478
-1.2812	-1.1742	2.0914	1.73024	1.0669447
0.01003	0.04517	0.04118	-0.1895	0.1749125
0.0095	0.04283	0.03962	-0.1786	0.1650325
0.00178	0.00821	0.00867	-0.0334	0.0311334
-1.2428	-2.586	-1.3165	1.85376	-2.947922
-0.0113	-0.0511	-0.0448	0.21896	-0.201594
-0.0105	-0.0473	-0.0426	0.19993	-0.184373
-0.0085	-0.0384	-0.0364	0.15886	-0.147006
0.01178	0.05317	0.04588	-0.2305	0.2119977
-0.0106	-0.0477	-0.0428	0.20164	-0.185919
0.00661	0.03004	0.02972	-0.1231	0.1141927
-0.0105	-0.0474	-0.0426	0.20013	-0.184551
0.00343	0.01574	0.01639	-0.0641	0.0596931
0.01129	0.05085	0.04463	-0.2177	0.2004865
-2.5443	0.36851	-1.5094	-1.5266	-1.53327
0.01095	0.0493	0.04374	-0.2097	0.1932074
-0.6543	-3.2171	-0.6493	-3.3582	-4.143373
0.01119	0.0504	0.04438	-0.2154	0.1983663
0.01115	0.0502	0.04426	-0.2144	0.1974326
-1.2375	1.46881	0.29563	0.82524	0.6191186
-0.0112	-0.0504	-0.0444	0.21519	-0.19818
0.01154	0.05202	0.04527	-0.224	0.2061818
0.00754	0.03419	0.03317	-0.1406	0.1303001
0.01131	0.05094	0.04468	-0.2182	0.2009425
0.01067	0.04805	0.04299	-0.2034	0.1875246
0.01109	0.04994	0.04411	-0.213	0.1961799
-0.0116	-0.0523	-0.0454	0.22541	-0.207418
-0.0114	-0.0512	-0.0448	0.21952	-0.202093
-0.0091	-0.0411	-0.0384	0.17092	-0.158007
0.01171	0.05283	0.0457	-0.2285	0.2102399
0.00803	0.03634	0.03487	-0.1499	0.1387735
0.66008	0.78999	-1.2981	-0.952	0.1908142
0.01157	0.05218	0.04536	-0.2249	0.2069867
0.01003	0.04518	0.04119	-0.1896	0.1749618
				-0.981773

## Appendix 8: Models training performance indexes

Hidden Layers	Levenberg-Marquardt			Bayesian Regularization			Scaled Conjugate Gradient			GPR			WBM		
	SSE	n	p	SSE	n	p	SSE	n	p	SSE	n	p	SSE	n	p
1	1531459.62	428	6	1854811.11	520	6	1597675.72	428	6	1100155.73	612	5	2208531.62	610	4
2	1361592.77	428	11	1225846.52	520	11	1433458.08	428	11						
3	987786.40	428	16	1128300.48	520	16	1588696.63	428	16						
5	1001434.75	428	26	1062629.94	520	26	1182222.11	428	26						
10	911378.72	428	51	852883.11	520	51	1135614.06	428	51						
15	665826.27	428	76	827958.21	520	76	1376715.62	428	76						
20	878556.95	428	101	828301.57	520	101	1011220.26	428	101						
40	600129.93	428	201	735619.62	520	201	1117642.89	428	201						
80	621370.89	428	401	724181.99	520	401	1191931.97	428	401						

H.L	Levenberg-Marquardt				Bayesian Regularization				Scaled Conjugate Gradient			
	AIC_LM	n/p	BIC_LM	RMSE_LM	AIC_BR	n/p	BIC_BR	RMSE_BR	AIC_SCG	n/p	BIC_SCG	RMSE_SCG
1	3944.4	71	3538.5	59.8	4787.5	86	4290.8	59.7	3962.5	71	3556.6	61.1
2	3473.8	38	3518.5	56.4	4582.6	47	4106.8	48.6	3495.9	38	3540.5	57.9
3	3346.5	26	3411.4*	48.0	4026.8	32	4094.9	46.6	3549.9	26	3614.8	60.9
5	3372.3	16	3477.9	48.4	4015.7	20	4126.3	45.2	3443.4	16	3548.9	52.6
10	3382.0	8	3589.0	46.1	3951.3	10	4168.3	40.5	3476.2	8	3683.2	51.5
15	3297.7*	5	3606.1	39.4	3985.9	6	4309.2	39.9	3608.6	5	3917.1	56.7
20	3466.3	4	3876.3	45.3	4036.1	5	4465.8	39.9	3526.5	4	3936.5	48.6
40	3503.2	2	4319.1	37.4	4174.4	2	5029.4	37.6	3769.3	2	4585.2	51.1
80	3918.1	1	5545.8	38.1	4566.3	1	6272.0	37.3*	4196.9	1	5824.6	52.8

\*Minimal value for each evaluation criterion

GPR				WBM			
AIC_GPR	n/p	BIC_GPR	RMSE_GPR	AIC_WBM	n/p	BIC_WBM	RMSE_WBM
5210.6	122	4618.6	42.4	5618.7	152	5024.2	60.2